

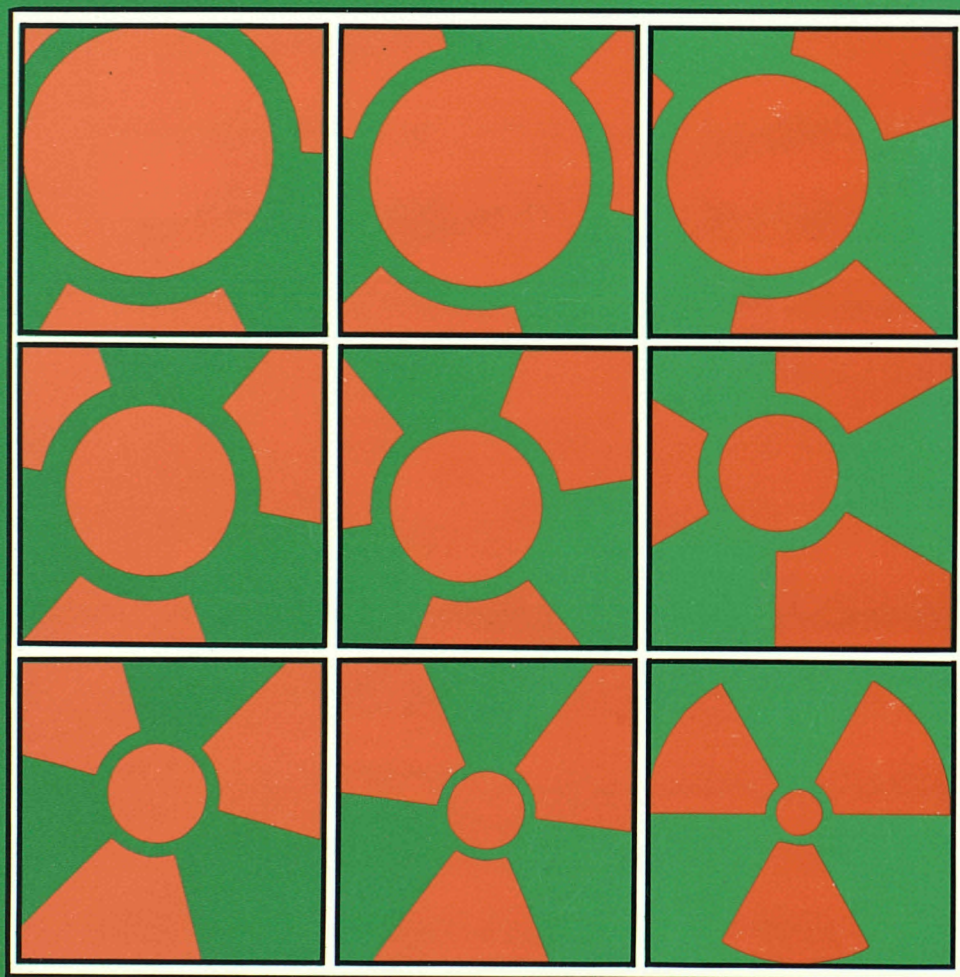
EUR 13.280



Commission of the European Communities

nuclear science and technology

**The uranium source-term mineralogy and
geochemistry at the Broubster natural
analogue site, Caithness**



Report

EUR 13280 EN

Commission of the European Communities

nuclear science and technology

The uranium source-term mineralogy and geochemistry at the Broubster natural analogue site, Caithness

A. E. Milodowski,¹ I. R. Basham,²
E. K. Hyslop,² J. M. Pearce¹

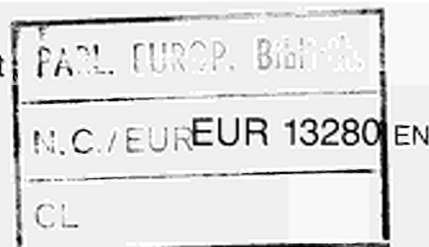
¹ **British Geological Survey,**
Keyworth, Nottingham NG12 5GG
United Kingdom

² **British Geological Survey**
Murchison House, West Mains Road
Edinburgh EH9 3LA
United Kingdom

Topical report

Work carried out under cost-sharing contract No F11W/0073 UK
with the European Atomic Energy Community,
in the framework of its third R&D programme on management
and storage of radioactive waste,
Part A, Task 4, 'Geological disposal studies'

Directorate-General
Science, Research and Development



1991

77434

**Published by the
COMMISSION OF THE EUROPEAN COMMUNITIES
Directorate-General
Telecommunications, Information Industries and Innovation
L-2920 Luxembourg**

LEGAL NOTICE

Neither the Commission of the European Communities nor any person acting on behalf of the Commission is responsible for the use which might be made of the following information

Cataloguing data can be found at the end of this publication

Luxembourg: Office for Official Publications of the European Communities, 1991

ISBN 92-826-2420-X

Catalogue number: CD-NA-13280-EN-C

© ECSC-EEC-EAEC, Brussels • Luxembourg, 1991

Printed in Germany

PREFACE

The British Geological Survey (BGS) has been conducting a co-ordinated research programme at the Broubster natural analogue site in Caithness, North Scotland. This work on a natural radioactive geochemical system has been carried out with the aim of improving our confidence in using predictive models of radionuclide migration in the geosphere. It has involved collaboration with the Harwell Laboratory for U/Th series analytical work, and with W S Atkins Engineering Sciences for modelling. The natural analogue work jointly carried out has been supported by the Department of the Environment from July 1986 to March 1989 and by the Commission of the European Communities from July 1988 to September 1989 under the CEC shared-cost action MIRAGE II Project.

This report is one of a series being produced from this effort and it concentrates on the mineralogical characterisation of the uranium distribution in the limestone unit considered as the 'source-term' in the natural analogue model. Other reports and papers listed below give further details of the programme but the one by Ball & Milodowski, in particular, contains much background information relevant to this report.

Broubster reports

1. 'Geochemical modelling of the Broubster natural analogue site, Caithness, Scotland' by D. Read of WS Atkins Engineering Sciences. British Geological Survey Technical Report WE/88/43 and DOE Report DOE/RW/89.005.
2. 'The development of portable equipment to study physical and chemical phases in natural waters' by N. Breward and D. Peachey. BGS Technical Report WE/88/25 and DOE Report DOE/RW/88.102.
3. 'The characterisation of organics from the natural analogue site at Broubster, Caithness, Scotland' by B. Smith, M. Stuart, B. Vickers and D. Peachey. BGS Technical Report WE/89/33.
4. 'The geological, geochemical, topographical and hydrogeological characteristics of the Broubster natural analogue site, Caithness' by T.K. Ball and A.E. Milodowski. BGS Technical Report WE/89/37 and DOE Report DOE/RW/89.069.

5. 'Sorption studies of uranium in sediment-groundwater systems from the natural analogue sites of Needle's Eye and Broubster' by J.J.W. Higgo, W.E. Falck and P.J. Hooker. BGS Technical Report WE/89/40 and DOE Report DOE/RW/89.072.
6. 'Uranium series disequilibrium studies at the Broubster analogue site' by G. Longworth, M. Ivanovch and M.A. Wilkins. 20pp. Harwell Report AERE-R 13609 (1989).
7. Read, D. and Hooker, P.J. 1989. The speciation of uranium and thorium at the Broubster natural analogue site, Caithness, Scotland. In Scientific Basis for Nuclear Waste Management. Materials Research Society, 127, 763-770.

CONTENTS

Sections		Page
1.	INTRODUCTION	1
2.	GEOLOGICAL BACKGROUND	1
2.1	REGIONAL SETTING	1
2.2	THE BROUBSTER SITE	5
3.	MINERALOGICAL AND PETROLOGICAL ANALYSES	6
3.1	METHODS	6
3.1.1	Sampling	6
3.1.2	Scanning Electron Microscopy (SEM)	6
3.1.3	Cathodoluminescence (CL)	7
3.1.4	Fission Track Registration	8
3.2	PETROGRAPHY AND GEOCHEMISTRY	9
3.2.1	Background Lithologies (sandstones and siltstones)	9
3.2.1.1	<i>Field characteristics</i>	9
3.2.1.2	<i>Mineralogical compositions</i>	10
3.2.1.3	<i>Petrography</i>	11
3.2.1.4	<i>Alteration</i>	13
3.2.1.5	<i>Uranium locations</i>	14
3.2.2	Broubster Laminated Limestone	15
3.2.2.1	<i>Field relationships</i>	15
3.2.2.2	<i>Sedimentary Petrography</i>	18
3.2.2.3	<i>Calcite veining</i>	21
3.2.2.4	<i>Other vein minerals</i>	23
3.2.2.5	<i>Uranium locations</i>	25
3.2.2.6	<i>Uranium mass balance</i>	32
4.	DISCUSSION	33
4.1	GENERAL	33

4.2	URANIUM ORIGIN AND THE PALAEOENVIRONMENT	33
4.2.1	The Lacustrine Model	33
4.2.2	Uranium	34
4.3	URANIUM IN THE BROUBSTER LAMINATED LIMESTONE	35
4.3.1	Deposition and Concentration	35
4.3.2	Diagenetic Redistribution	36
4.3.3	Tectonic Remobilisation	40
4.3.4	Supergene Redistribution	41
4.4	DEFINITION OF THE BROUBSTER SOURCE TERM	41
5.	CONCLUSIONS	43
6.	ACKNOWLEDGEMENTS	46
7.	REFERENCES	46

Tables

1.	Middle Old Red Sandstone stratigraphy in the Broubster area	3
2.	Sample depths, nominal relative γ -activity and U and Th contents in quarry samples	10
3.	Sequence of calcite formation and cathodoluminescence characteristics	23
4.	Uranium contents determined by fission track counting, modal compositions and derived mass balances for uranium for two samples of the Broubster limestone	32
5.	Summary of relationships between diagenesis and uranium mineralisation in the Broubster laminated limestone	39

Figures

1.	Location map of Broubster Natural Analogue Site, Caithness and its relation to the distribution of the Middle Old Red Sandstone outcrop.	2
2.	Schematic profile of PIT 1, showing analytical data for uranium and thorium	17

EXECUTIVE SUMMARY

Supported by the Department of the Environment from July 1986 to March 1989 and by the Commission of the European Communities from July 1988 to September 1989 under the shared-cost action MIRAGE II Project, the British Geological Survey (BGS) has been conducting a number of investigations of locations where natural analogues of radionuclide migration can be recognised. The purpose of the research is to describe the processes of movement of uranium, thorium and rare earth elements in sediments, in order to provide data which can be used in modelling and testing applications of the CHEMVAL thermodynamic database and of transport codes such as CHEMTARD. Testing with real geological situations in this way can create confidence in the use of such codes as predictors of radionuclide transport in performance assessments of radioactive waste repositories.

The Broubster Natural Analogue site presents an accessible locality with relatively simple geology and groundwater system, in which particular emphasis can be placed on the study of the role of organics in soils and peat in the transport and fixation of uranium. The primary uranium mineralisation or "source-term" from which uranium has been mobilised is considered to be a unit of laminated limestone, about 40cms thick, interbedded with organic-silt beds of the Lybster Subgroup of the Lower Caithness Flagstone Group of the Caithness Middle Old Red Sandstone. The limestone appears to persist along strike throughout the analogue site and is significantly enriched in uranium compared with the background flagstone lithologies in the immediate area.

Detailed determination of the distribution and mineralogical character of uranium in the "source-term" is required in order to assess susceptibility to remobilisation by weathering and leaching. This has been accomplished by the integration of a variety of mineralogical methods. Autoradiographic and uranium fission track techniques have been used to locate uranium in levels ranging from a few to several hundred ppm, identification of the host phases being made subsequently by optical and scanning electron microscopy. Fission track registration has also allowed quantitative determination of mass balances of uranium in the limestone, in order to assess potential contributions from host phases of differing leachability. Optical and scanning electron microscopy, coupled with cathodoluminescence, have also been applied in the petrogenetic study of the origin and evolution of uranium within the rock system, in order to evaluate the behaviour under varying conditions through geological time. Samples examined were obtained principally from a pit dug over the strongest radiometric anomaly in the site but representative background samples were also collected in order to establish the nature of the processes responsible for the concentration of uranium in the limestone.

The investigation has revealed a complex history of uranium deposition and redistribution within the laminated limestone unit during a sequence of distinct geological events. Uranium mobility can be considered in relation to its origin within the palaeoenvironment of the deposition of the sediments of the Orcadian lake, followed by mechanisms of fixation and concentration in the sediments and subsequent diagenetic and tectonic remobilisation and redistribution. The cumulative effects of these processes determine the ultimate host phases of uranium, thereby governing leachability in the present-day weathering regime.

The limestone is composed of repeated triple units comprising bands of recrystallised carbonate mud (microsparrite), very fine organic-rich silty-clay lamellae and coarser clastic lamellae. These units are generally less than 1mm thick, the carbonate bands predominating in volume by a factor of about 7:1. The uranium in the limestone was derived from weathering of mainly granitic basement rocks in the provenance areas of the Flagstone Group sediments and is considered to have been introduced syngenetically into the sedimentary environment in solution, colloidal suspension and, to a minor extent, as detrital minerals. Seasonal life cycles of algae/cyanobacteria which developed and proliferated in the upper (euphotic) waters of the Orcadian lake have been of critical importance in the formation of the limestone and are considered to have been the principal factor in the early fixation of uranium. Precipitation of the carbonate bands is related to algal growth and the accumulation of evenly dispersed uranium in this lithology, most probably held by substitution in the carbonate crystal lattice, is considered to be contemporaneous with formation or related to very early diagenetic recrystallisation. During this process soluble U^{6+} (probably present in solution as a bicarbonate complex) possibly coprecipitated with Ca^{2+} from the lacustrine waters as a result of algally (photosynthetic)-induced carbonate ($CaCO_3$) precipitation during the seasonal algal blooms. Consequently, uranium has been concentrated in the carbonate sediment bands in levels up to 30ppm but Th, which would not have been present in the upper lake waters as a soluble complex, has not been enriched by these processes. Early subaerial alteration has modified part of the limestone unit, with loss of uranium from the system during calcrete-type recrystallisation of carbonate.

Within the organic-silt laminae, in addition to minor input from detrital heavy minerals, the major part of the uranium can be accounted for by either:

- 1) syngenetic concentration of uranium from euphotic lacustrine waters at the margin of the Orcadian Lake by living algae/cyanobacteria and accumulation within the sediment upon their death, or;
- 2) fixation of uranium within the eodiagenetic organic-rich reducing environment of the sediments from uranium-charged refluxing lake margin groundwaters.

Part of this organically-fixed uranium remains in association with biologically mineralised

early diagenetic "hydrocarbon globules" as discrete included minerals. However, the major location of uranium in quantitative terms is a variety of finely divided diagenetic minerals, including phosphates, intimately associated with framboidal pyrite. Some uranium may possibly be associated with finely dispersed amorphous organic matter (of algal origin) which is abundantly present in these silt laminae and within which the pyrite has developed. This dispersed uranium attains levels of up to 60ppm. Thorium and rare earth elements are also enriched in this lithology, frequently in association with the uranium.

Late or post-diagenetic redistribution of uranium has been of minor extent. Several successive generations of tectonically-related complex calcite veining have affected the limestone unit pervasively, but the only event which appears to have involved significant mobilisation of uranium, was a phase of polymetallic mineralisation. Introduction of copper, zinc and lead as sulphides, together with pyrite and a trace of gold, was accompanied by formation of calcite and baryte and migration and emplacement of liquid hydrocarbons with redistribution of uranium into the mineralised fractures. This uranium, though of minor significance quantitatively, appears to be relatively labile although some of these secondary uranium minerals in hydrocarbon-filled vuggy cavities may effectively be rendered immobile where they are protected from dissolution in the present groundwaters by the highly insoluble hydrocarbons. Unlike the early diagenetic hydrocarbon globules this later vein hydrocarbon has not suffered uranium biomineralisation. The calcite gangue in the veins, which make up 15-20% of the rock, contain negligible dispersed or lattice-held uranium.

In summary, the two principle lithologies within the limestone unit have been shown to contain uranium in different associations. These were established at a very early stage in the formational history of the limestone and have been notably stable over considerable time and through a variety of geological conditions. Present-day release mechanisms are different but related :-

The organic-silt laminae represent around 10% of the source-rock and contain around 20% of the total uranium. The bulk of this appears to be contained in very fine grained composite diagenetic minerals, often in association with rare earths and occurring intimately intergrown with weakly soluble minerals. However, the close spatial relationship to dispersed diagenetic pyrite has allowed some degree of oxidation and mobilisation of uranium concomitant with pyrite oxidation. Acidic solutions generated by this reaction probably play an important role in this respect. Uranium associated with sedimentary carbonate accounts for 80% of the total, contained in around 75% of the limestone. As this appears to be held in the carbonate lattice (or as a sub-crystalline dispersed phase), liberation into solution necessitates bulk rock dissolution. This mechanism is evidently active at the present day in percolating acidic groundwaters, uranium presumably being mobilised as the bicarbonate

complex. Although some evidence has been found of local re-precipitation, this is not considered to be extensive.

Although the dominant carbonate-band lithology of the limestone contains only low levels of thorium and rare earth elements, the organic-silt laminae and the enclosing siltstone lithologies show appreciable enrichment. Investigation of these is merited in order to assess them as possible "source-terms" in analogue modelling based on these elements, as well as to study further their role in supergene release of uranium.

1. INTRODUCTION

It is important to test applications of the CHEMVAL thermodynamic database and transport codes such as CHEMTARD with real geological situations in order to create confidence in their use as predictors of radionuclide transport in performance assessments of radioactive waste repositories. To this end the British Geological Survey (BGS) has been conducting a number of investigations of locations where natural analogues of radionuclide migration can be recognised, with the purpose of describing the processes of movement of uranium, thorium and rare earth elements in sediments. In this way, data can be compiled to be used in modelling and testing the inherent ideas in the codes. The uranium mineralisation at the Broubster Natural Analogue site presents an easily accessible locality suitable for such a study with the emphasis on the role of organics in the transport and fixation of uranium. This report concentrates on the mineralogical aspects of the primary uranium mineralisation or "source-term" from which uranium has been mobilised. The report compiles new results and presents a comprehensive information base for modelling aqueous uranium speciation and transport.

2. GEOLOGICAL BACKGROUND

2.1 REGIONAL SETTING

The Broubster site (National Grid Reference ND 021 624) is located inland of the north coast of Caithness, about 11km southwest of Thurso and 6km southeast of the Dounreay Experimental Reactor Establishment (Figure 1). The mineralised structure was discovered in the course of regional radiometric and hydrogeochemical surveys (Gallagher et al, 1971) and occurs within the Lybster Subgroup of the Lower Caithness Flagstone Group of the Middle Old Red Sandstone (MORS) of north Caithness. Regional stratigraphic relationships (based on Donovan et al, 1974; Mykura, 1983; BGS 1985) are shown in Table 1.

The MORS of northeast Scotland is dominated by lacustrine sediments (Donovan, 1975; 1978; 1980; Donovan et al, 1974; Mykura, 1983) laid down within an enclosed northeast trending continental basin (the Orcadian Basin) made up of a series of connected but distinct half-graben sub-basins (Norton et al, 1987). A possible connection between the Orcadian lake and the sea existed in the middle of the present North Sea area (Kent, 1975 ; Mykura, 1983). The eastern margin of the lake is

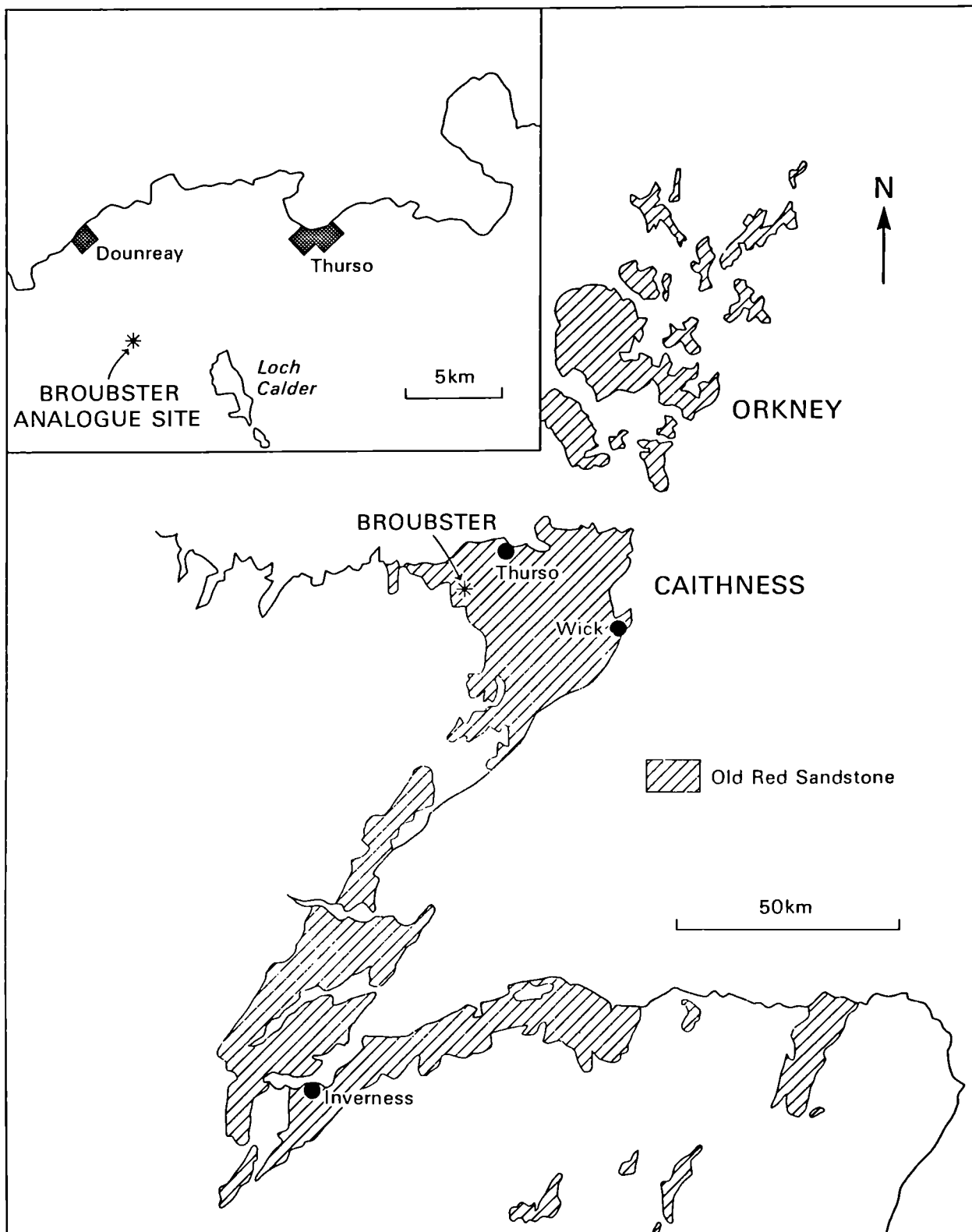


Figure 1: Location map of the Broubster Natural Analogue Site, Caithness and its relation to the distribution of the Middle Old Red Sandstone outcrop.

uncertain but the western margin probably corresponded closely to the present western limit of the Caithness Flags outcrop (Mykura, 1983). Further west the MORS is represented by relicts of fluvial conglomerate and sandstones deposited from rivers draining the mountainous metamorphic and igneous terrain to the west of the Orcadian lake (Blackbourn, 1981).

Table 1. Middle Old Red Sandstone stratigraphy in the Broubster area

Middle Old Red Sandstone

John O' Groats Sandstone Group

Upper Caithness Flagstone Group

Mey Subgroup

Ham-Scarfskerry Subgroup

Latheron Subgroup/Spittal Subgroup

Achanarras and Niandt Limestone Member

Lower Caithness Flagstone Group

Robbery Head Subgroup (not recognised in this area)

Lybster Subgroup

Hillhead Red Bed Subgroup (not recognised in this area)

Clyth Subgroup/Berriedale Flagstone Formation/undifferentiated sandstone
(± basal breccia)

Barren or Basement Group/Sarclat Group

Basal conglomerate. Angular unconformity in south and west Caithness.

The lacustrine Caithness Flags throughout comprise a monotonous cyclical series of sediments that represent seasonally controlled sedimentation superimposed upon repeated longer-term transgressive and regressive cycles in lake level. Four distinct lithological associations or facies are distinguished within these cycles (Donovan 1980) and are present in the Broubster area :

Facies A

Laminated sediment dominated by carbonate which may form limestone horizons. They comprise micritic carbonate (dolomite or calcite), organic carbon and clastic lamellae which form a triplet averaging 0.5mm in thickness. The clastic lamellae are composed of silt-grade detrital quartz, feldspar, chlorite, muscovite and biotite in a matrix of illite and chlorite clay

minerals. The organic lamellae are very fine and sometimes indistinct from the clastic lamellae. These sediments are pyritic, contain fish remains and commonly form fish beds. They are interpreted as seasonal varves in a tropical eutrophic lake where the waters were subject to some degree of seasonal thermal stratification. "Summer" algal blooms in the upper, warm, productive euphotic waters (epilimnion) caused the precipitation of carbonate and when the algae died ("autumn") they accumulated on top of the carbonate sediment in the anaerobic lake bottom waters (hypolimnion). The clastics may represent either a continuous background sedimentation or terrigenous input during wetter seasons ("winter"). These laminite limestones were developed close to the edge of the basin where the waters were warmer and algal activity more prolific (Donovan, 1975). They represent periods when the Orcadian lake was at its deepest and its margin coincided with the basin margin (Donovan, 1975). Landwards, in shallower waters these laminites pass into more massive limestones, stromatolitic deposits and eventually into calcreted horizons which may interdigitate with fluvial deposits (Donovan, 1973; 1975; Parnell, 1983). Basinwards they pass into more typical dark grey and more clastic-rich flagstone facies.

Facies B

Laminated sediments consisting of dark-grey, organic carbon-rich siltstone and shale laminae. The thickness of laminations varies between 0.5 to 3.0mm. Distinct carbonate bands are fewer, although small amounts of micrite are present in some shale laminae. Syndimentary gas-escape structures ("mound structures", Donovan & Collins, 1978) are common and some subaqueous shrinkage cracks (Donovan & Foster, 1972) are present. Sedimentary conditions are interpreted as a shallow productive largely permanent lake environment but mostly under quiet conditions below the wave base, in which sediment supply was restricted. Seasonal stratification of the lake was not well developed and consequently carbonate precipitation was limited.

Facies C

Alternations of dark grey carbon-rich shale and coarse grey siltstone laminae in pairs averaging 10mm thickness. The siltstone laminae often show single-set ripple cross-bedding; sequences of this type greatly resemble lenticular bedding. Subaqueous shrinkage cracks are common but subaerial shrinkage cracks are rare. These sediments are thought to have formed in shallow, occasionally dessicated lakes in which water level and salinity fluctuated periodically (possibly seasonally). The repetition of siltstone and shale is possibly the result of surface wave action during seasonal fluctuations in lake level.

Facies D

Alternations of variously hued (dark grey, light grey, grey green, dark olive green) shales with siltstones and fine sandstones in discrete beds from 1 to 100mm in thickness. Coarser sediments show abundant multi-set ripple cross bedding which resembles flaser bedding and many surfaces display symmetrical ripples. Subaerial shrinkage cracks are common but subaqueous shrinkage cracks are restricted to darker shales. Pseudomorphs after gypsum or other evaporites are occasionally present (Parnell, 1985(a)). These sediments are considered to have formed in a shallow temporary lake environment (lake flats) and locally may have been influenced by periods of fluvial sedimentation. This facies developed at the lake shoreline during the early stages of lake transgression.

Thin dolomicrite beds up to 5cm thick may be developed in facies B,C and D and some appear to have formed as crusts on the sediment surface. These may in part represent sabkha conditions (Donovan, 1978) or stromatolitic deposits (Parnell, 1988).

2.2 THE BROUBSTER SITE

The main features of the geology of the Broubster Natural Analogue site, together with a summary of earlier work and new results from hydrogeological and geochemical studies, are described in detail in a companion report by Ball & Milodowski (1989). Radiometric and geochemical investigations reveal a complex pattern of uranium transport and dispersion downslope from a source where bedrock is close to surface on the west side of the site into a peat-bog which overlies boulder clay to the east. Gallagher et al (1971) considered the source to be at the site of an old limestone working (now largely backfilled) and from study of this, supported by limited drilling, reported the occurrence of fault-bounded vein mineralisation with a northeast trend hosted by a bed of bituminous limestone with similar strike and gentle dip to the north. Although the mineralisation was found to comprise calcite with dolomite, sphalerite, galena and globules of uraniferous hydrocarbon, it was suggested that the bulk of the uranium and other metals in the secondary concentration in the peat was probably derived from the limestone itself. The presence of a weakly uraniferous black siltstone horizon to the northeast of the old workings was also noted.

The secondary dispersion pattern closely follows the local drainage pattern of the site with an elongation following a surface drainage channel flowing to the northeast. Ball & Milodowski (1989) also consider that, in the northeast of the present research area where boulder clay cover appears to be absent, there is the potential for a possible recharge of "fresh" uranium into the dispersion pattern evolved within the peat horizon. This addition of

uranium to the system may arise either directly from bedrock or from an extension along strike of the mineralisation seen in the west, or from groundwater outflowing from the boulder clay-bedrock interface. Any uranium in this groundwater will have evolved along a different pathway from the uranium in groundwater moving within the peat layer.

3. MINERALOGICAL AND PETROLOGICAL ANALYSES

3.1 METHODS

3.1.1. Sampling

Outcrop exposure in the study area is limited and samples for petrographical and mineralogical characterisation of the uranium source and background lithologies were obtained principally from small excavated pits. Details of the locations and their geological and hydrogeological relationships within the analogue site as well as results of chemical analysis of selected samples are given in Ball & Milodowski (1989). The source mineralisation was accessed in PIT 1 which was located over the strongest radiometric anomaly in the old limestone working on the west side of the site. For comparison, background samples of sandstone and siltstone were obtained from a small, recently worked but now disused quarry about 100m southeast of the old limestone working.

Representative subsamples were ground for chemical analysis, procedures and results being given in Ball & Milodowski (1989). Chemical data referred to in this report are taken from that source. Polished thin sections for mineralogical and petrological study were prepared by conventional methods including prior impregnation with a coloured (usually blue) epoxy resin in order to highlight and distinguish porosity.

3.1.2 Scanning Electron Microscopy (SEM)

Scanning electron microscope (SEM) analysis was undertaken using a Cambridge Instruments Stereoscan S250 scanning electron microscope fitted with a 4-element solid-state (diode) backscattered electron detector (KE Developments Ltd). Mineralogical and chemical characterisation of phases imaged under the SEM was facilitated by qualitative observation of their energy-dispersive X-ray spectra. These were recorded using a Link Systems 860 energy-dispersive X-ray microanalyser (EDXA). The EDXA system has a detection limit of approximately 0.2 % (weight) for most common elements but this is probably of the order of 0.5% (weight) for uranium, thorium and other heavy elements at typical count-times of 100

seconds at 20kV.

Analysis was carried out using both ordinary stub-mounted (rough surface) specimens and polished thin-sections. Observations of rough stub-mounted specimens were made by routine secondary electron imaging techniques which provide largely morphological information by imaging the low-energy secondary electrons produced in the specimen surface by interaction between the primary electron beam and the sample. The image brightness or shadowing depends largely upon the orientation of the surfaces being examined in relation to the electron detector. Polished thin-sections were studied in backscattered electron imaging mode (BSEM) in which images are related to the composition of the material being examined. Image brightness is proportional to the average atomic number of the material, thus allowing the distribution of different minerals or phases to be determined on the basis of their chemical composition. Although irregularities on a specimen surface can affect the interpretation of BSEM images, the technique can nevertheless be extremely useful in the location of dense trace minerals (which show up as bright grains) even in rough surfaces. BSEM has been used very effectively in the study of sediment diagenesis, mineralisation and alteration (eg Krinsley et al, 1983; Huggett, 1984; Pye & Krinsley, 1984; Strong & Milodowski, 1987).

Prior to SEM examination the sections were coated with a thin film of carbon (approximately 200Å) by evaporation onto the section surface under vacuum. Rock-chips were similarly carbon-coated after being first mounted on aluminium pin-type SEM stubs using Leit-C conducting carbon cement. All SEM observations were carried out at 20kV beam potential.

In order to identify the phases containing uranium systematically, comparison of the SEM images was made with fission-track prints (Section 3.1.4). Enlargements of these were made by microfiche xerox-copier in order to produce a large-scale "map" of the uranium distribution for each polished section. From such maps it was possible to locate the uranium-bearing phases accurately and rapidly under BSEM in order to identify them by EDXA and determine their petrogenetic relationships.

3.1.3 Cathodoluminescence (CL)

The phenomenon of the emission of light from certain minerals (eg carbonates) during electron irradiation (cathodoluminescence) has been summarised by Nickel (1978). Cathodoluminescence (CL) has its origin in the molecular distortions of the crystal lattice. These structures give resonance under electron bombardment, but radiation is also controlled by the very complex balance of valence electrons in a crystal lattice. These resonating

valence bands may be related to:-

1. Distorted surfaces (eg stress cracking)
 2. Distorted internal structure between intergrown crystals
 3. Hole defects (atoms or ions missing from the lattice)
 4. Inhomogeneities in composition
 5. Impurities (trace elements) in surface sites, regular lattice sites or interstitial sites
 6. Charge displacements, abnormally ionised atoms, separated cation-anion pairs
- All these imperfections affect the energetics of the crystal lattice.

Therefore CL can provide a useful tool for the distinction or correlation of mineralisation features due to similarities or differences in their geochemical or tectonic paragenesis or for revealing the original fabric in recrystallised rocks (eg Sippel, 1968; Meyers, 1974; Grover & Read, 1983; Strong & Milodowski, 1987). CL is particularly useful in the study of carbonate minerals. In this case, CL activity is considered to be due mainly to variations in trace amounts of iron and manganese (Pierson, 1981; Walker et al, 1989). Manganese is believed to cause CL excitation whereas iron in excess of about 1% drastically quenches CL emission. It should be noted however, that CL zonation can reflect the composition and degree of saturation of the precipitating fluid as well as crystal growth rate. Consequently CL variations do not necessarily indicate wide differences in fluid composition (Ten Have & Heijnen, 1985).

CL observations were made on polished thin-sections of sandstone and limestone using a Technosyn model 8200 MkII cold cathode cathodoluminescence stage fitted to an optical microscope with long working-distance objective lenses. The instrument was operated at an excitation voltage of 10-20kV and a beam current of 500-700 μ A. Care had to be taken in order to prevent the destruction of the sample during observation. CL images were photographically recorded with 35mm fast colour film (Kodacolor VR 1000ASA).

3.1.4 Fission Track Registration

Uranium and thorium occur naturally in rocks in a great variety of host phases and in a wide range of concentrations (e.g. Basham, Ball, Beddoe-Stephens & Michie, 1982(a)). In any comprehensive mineralogical and geochemical study of radionuclide occurrence and distribution, the location of all possible hosts by charged particle track registration techniques is an essential precursor to evaluation by identification methods such as optical and electron microscopy. In this study, preliminary evaluation of the distribution of overall radioactivity was made by registration of natural alpha particle activity in polished thin sections in CR39

plastic, following the procedures described by Basham (1981). However, as this technique does not allow ready discrimination between uranium and thorium series nuclides, the precise location of all uranium sites was achieved by recording fission fragments derived from uranium under neutron irradiation in a reactor [(n,f) reaction]. Interference from thorium was avoided by selecting a highly thermalised neutron flux in which only ²³⁵U undergoes appreciable fission. Irradiations were carried out at the Scottish Universities Research and Reactor Centre, East Kilbride.

The method employed was based on that of Kleeman & Lovering (1967). "Lexan" polycarbonate plastic was used as a detector and tracks of the induced fission fragments revealed by etching for 5 minutes at 60°C in 6 molar NaOH solution. The technique yields accurate spatial information on the location of uranium in the sample in the form of micromaps. Quantitative estimation of the uranium content of different host minerals was achieved by the irradiation of uranium-doped standard glasses along with the sample batches and consequent track counting on an equal area basis using an optical microscope. Neutron fluence was chosen to yield discrete tracks with minimum overlap to ensure reasonable counting accuracy (typically 2×10^{15} t.n.cm⁻² is used). In some cases it was found necessary to make more than one fission track registration "print" at different neutron fluences in order to obtain workable track densities or to increase sensitivity. In this way, uranium contents in the range 1 to several 100s ppm were measured with good reproducibility. Data obtained were used in coordination with modal estimates of phase abundance to derive mass balances for uranium in the samples.

3.2 PETROGRAPHY AND GEOCHEMISTRY

3.2.1 Background Lithologies (sandstones and siltstones)

3.2.1.1 *Field characteristics*

In order to establish the background lithology and geochemistry to the source-term location, four samples of sandstone and siltstone (Latherton Subgroup, Upper Caithness Flagstone Group; Table 1) were collected from the small forestry quarry to the southeast of the site. In this area boulder clay cover is absent and a thin peat blanket rests directly on gently dipping flagstones. About 1.5m of bedrock was accessible and the sample depths (relative to the bedrock top) and nominal total γ count at these depths are given in Table 2, along with the analytical data obtained for uranium and thorium. The total γ -activity varies largely with uranium content but the "anomolously" higher γ -count in BR09/4 for its relatively low

uranium content is probably due to the solid angle effect on the γ -detector at the base of the quarry profile.

Table 2. Sample depths, nominal relative γ -activity and U and Th contents in quarry samples

SAMPLE	DEPTH (cm)	γ - ACTIVITY (cps)	U(ppm)	Th(ppm)
BR09/1	0	75-85	3	8
BR09/2	30	130-140	7	9
BR09/3	45-50	105	5	8
BR09/4	150	95-105	2	5

The samples examined are strongly weathered displaying a buff or orange-yellow to rusty-brown colour and were quite friable. BR09/1, BR09/3 and BR09/4 are all very similar and comprise ochreous fine ripple cross-bedded medium to fine sandstones with occasional thin laminae of silty mudstone. Sandy laminae are 3 - 10mm in thickness with thinner mudstone laminae typically 0.2 to 2mm thick. BR09/2 is more typical of flagstone lithology, consisting of more finely laminated siltstone or mudstone and sandstone with 0.1 - 2mm laminae. Despite the strong weathering, relicts of fine black organic laminae are seen on bedding planes and traces of low-angle cross-bedding are also apparent. In all specimens vertical fractures and bedding planes are commonly coated with secondary iron oxide(s), probably goethite. In BR09/1 and BR09/2 this is hard, dense and dark red-brown whereas in BR09/3 and BR09/4 the coating is powdery and of yellow ochre colour.

3.2.1.2 Mineralogical composition

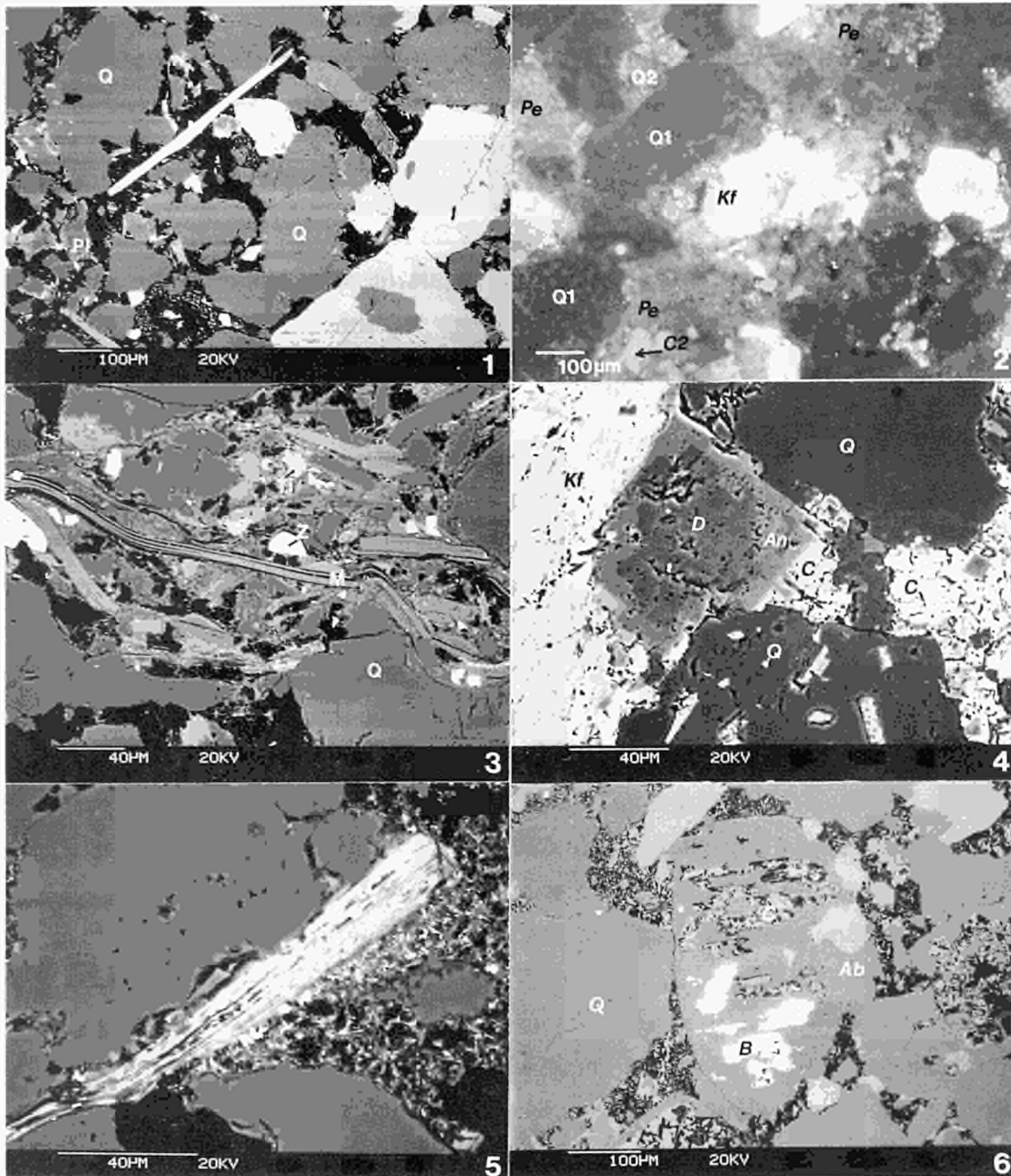
Mineralogically, the samples are similar and composed largely of detrital quartz, with subordinate K-feldspar, plagioclase, muscovite, chlorite, biotite and mudstone pellets. Lithic clasts comprising granoblastic intergrowths of quartz, K-feldspar, albite and muscovite are common and probably represent material derived from granitic terrain. Silty clay and fine

siltstone laminae also contain a matrix of fine-grained mica (illite) and possible chlorite or mixed-layer chlorite-smectite. Although no confirmatory X-ray diffraction analysis of the argillaceous matrix has been performed, these observations are consistent with published data for the clay mineralogy of the MORS of Caithness (Wilson, 1971) which indicate a clay assemblage dominated by illite and chlorite, at times including minor illite-smectite mixed-layer species in the mica component. Accessory detrital phases include common zircon, rutile and apatite with rarer chromite, a spinel (intermediate between chromite, spinel, hercynite or magnesioferrite), monazite and very rare xenotime.

3.2.1.3 Petrography

The sandstones and sandstone laminae are extremely porous and possess a largely grain-supported fabric (Plate 1). A rigid framework has been provided by extensive precipitation of interlocking authigenic quartz and K-feldspar as overgrowths seeded on the detrital grains. Cathodoluminescence reveals that overgrowth occurred in an open detrital fabric with simple grain contacts and without grain stress-cracking, pressure-solution or sutured grain boundaries (Plate 2). Together with the absence of compactional deformation in the less competent micas (Plate 1), these features suggest that a rigid framework, cemented by authigenic quartz and K-feldspar was established at an early diagenetic stage, prior to significant burial and compaction. In contrast, the argillaceous laminae consist of closely compacted sediments with limited or no grain overgrowth cements. Within these laminae, the detrital micas are usually deformed and compacted around quartz and feldspar clasts (Plate 3).

Elsewhere in north Caithness (Basham & Milodowski, unpublished data), the Caithness Flagstones are often pyritic and extensively cemented by carbonates. In this study, carbonates and pyrite have been noted only in the deepest sample (BR09/4) examined from the disused sandstone quarry, the Broubster laminated limestone (see 3.2.2) and in loose fragments of flagstone present in the drift deposits. Sample BR09/4 contains preserved pyrite in relict patches of carbonate cement consisting of moderate-to-brightly yellow luminescent, non-ferroan or weakly ferroan calcite (Plate 2) filling intergranular sites (pore-filling) and framework grain dissolution (FGD) sites (mainly after feldspar).



- PLATE 1. BSEM photomicrograph showing grain supported detrital fabric of porous sandstone. Consists of detrital quartz (Q), K-feldspar (Kf), muscovite (M), and plagioclase (Pl). Note lack of mica deformation, presence of corroded plagioclase and intergrowth of quartz. BR09/4.
- PLATE 2. CL photomicrograph of sandstone showing uncompact grain-supported fabric of non luminescent detrital quartz (Q1) and blue-luminescent feldspars with pore-filling bright-yellow luminescent calcite cement (C2). Note dull-luminescent quartz overgrowths (Q2) forming interlocking grain fabric. Dull orange luminescent detrital carbonate pelloids (Pe) also present. BR09/4.
- PLATE 3. BSEM photomicrograph of silty clay lamination in flagstone displaying burial-compaction deformation of detrital muscovite (M). Micas aligned parallel to bedding. Detrital zircon (Z) and fine secondary TiO₂ (Ti) also seen in clay matrix. BR09/4.
- PLATE 4. BSEM photomicrograph showing syntaxial overgrowth of ankerite-ferroan dolomite (An) on detrital dolomite carbonate grain (D). Calcite cement (C) and detrital quartz (Q) and K-feldspar (Kf) also shown. BR09/4.
- PLATE 5. BSEM photomicrograph of altered detrital biotite showing basal expansion of flake and fine precipitates of plumbogummite minerals, TiO₂ and goethite along cleavage. Fine (bright) goethite coating clays seen in adjacent porosity. BR09/2.
- PLATE 6. BSEM photomicrograph of albitised detrital plagioclase (Ab) with FGD sites infilled by baryte (B) and calcite (C). BR09/4.

Also present are relatively large areas of calcite cement which are oversized in comparison to the normal intergranular regions and are characteristic of the replacement of former detrital grains or infilling of FGD sites (Schmidt & McDonald, 1979). The calcite cement encloses and partly replaces or corrodes authigenic quartz and feldspar and therefore post-dates quartz and feldspar authigenesis.

Within the calcite-cemented areas, rounded detrital carbonate clasts are abundant and comprise both dull-luminescent micritic calcite (Plate 2) and easily distinguishable, red luminescent micritic or recrystallised ferroan dolomite. The dolomite clasts usually exhibit syntaxial overgrowth (if recrystallised) or partial replacement by ankerite or strongly ferroan dolomite (Plate 4). Dolomite cements also invade and replace detrital mica along cleavage, causing expansion and splitting of the flakes. Ankerite is either intergrown with, or slightly replacive towards quartz and feldspar authigenic overgrowths, indicating either syngenetic or slightly later formation. These authigenic dolomite-ankerite cements are in turn partly replaced by the calcite cement discussed above. Pyrite commonly occurs in finely disseminated around the micritic dolomite clasts or as dispersed framboidal aggregates. Detrital apatite is a common minor constituent in the cemented rock and is seen to be rimmed by minor authigenic overgrowth.

3.2.1.4 *Alteration*

Extensive alteration of these sedimentary rocks is probably attributable in the main to weathering processes. The porosity in the sandstones is largely secondary as a result of the dissolution of calcite, dolomite and ankerite cements and, to a lesser extent, the dissolution of detrital and authigenic feldspars (Plate 1). Apatite is also etched and corroded in carbonate-free rock and pyrite, where not preserved within the relict carbonate cement, is represented by goethite pseudomorphs. Very fine grained goethitic iron oxide is also abundantly present as coatings on mineral surfaces within the secondary porosity (Plate 5).

Other secondary minerals are present, including anatase, baryte and minerals of the plumbogummite group. In many cases it is not possible to assign these minerals specifically to either diagenetic or weathering processes. Microcrystalline anatase or amorphous TiO_2 is particularly abundant and in some cases is intimately associated with goethite in secondary porosity, most probably as a product of weathering. Elsewhere, coarser crystalline anatase occurring in both cemented and uncemented rock as an alteration product of detrital grains (probably former ferromagnesian and Fe-Ti oxide minerals) is more likely to be of early diagenetic origin. Similarly, baryte may be associated with goethite as a fine admixed alteration along bedding lamellae but also occurs as an early diagenetic mineral precipitated in

FGD sites and enclosed in, or associated with, later calcite cement (Plate 6).

The plumbogummite group minerals are associated with sites of mica alteration, in particular biotite, accompanying secondary iron and titanium oxides precipitated along cleavages (Plate 5). They range in composition from goyazite ($\text{SrAl}_3\text{H}(\text{PO}_4)_2(\text{OH})_2$) to a mineral intermediate between goyazite and florencite ($(\text{Ce,La,Nd})\text{Al}(\text{PO}_4)_2(\text{OH})_6$). Ce is the dominant REE in most examples of florencite-goyazite and sometimes the only REE detectable by BSEM-EDXA. Alteration to material of rhabdophanic composition ($(\text{Ce,La,Nd,Th,Ca})\text{PO}_4 \cdot n\text{H}_2\text{O}$) is also sometimes present around rare detrital monazite grains. Rare possible witherite (BaCO_3) is found in the most weathered sandstone samples (BR09/1, BR09/2). As these less common minerals have not been observed in the unweathered carbonate cemented rock they are considered to be products of supergene alteration.

In view of the altered state of the specimens examined, it is difficult to assign these sandstones precisely within the lacustrine facies defined by Donovan (1980). On the basis of the grain size, lack of shale and presence of ripple cross-bedding, the most probable facies to which these sediments belong is either Facies "C" or Facies "D".

3.2.1.5 Uranium locations

Whole rock values for uranium and thorium range from 2-7ppm U and 5-9ppm Th (Table 2). These levels do not indicate significant enrichment and suggest that uranium and thorium are located principally in detrital heavy minerals. Although no autoradiographic or fission track analyses have yet been conducted on these sandstones it is likely that some redistribution will have occurred at least during the supergene alteration described above. In BSEM-EDXA examination, uranium was detectable only in rare detrital xenotime although other detrital minerals present such as zircon, apatite and monazite undoubtedly contain uranium, albeit below detection level. Thorium was detectable in significant amounts in rare detrital monazite and associated rhabdophanic alteration but the characteristic X-ray lines for any uranium present in these minerals would probably be obscured by thorium lines.

Recognition of detrital minerals as principal hosts for the low levels present, together with limited evidence of very local redeposition during weathering, indicates that these sandstones are not to be considered as potential sources of appreciable uranium and thorium.

3.2.2 Broubster Laminated Limestone

3.2.2.1 *Field relationships*

Limestone and associated mineralisation were accessed by a shallow pit (PIT 1) dug in the area of the old limestone workings. The pit profile is shown in Plate 7 and illustrated schematically in Figure 2, annotated with pertinent analytical data for uranium and thorium. A thin (approximately 40cm) bed of brownish grey, finely laminated limestone with abundant siltstone laminations, dips gently northwards at the base of the pit. The basal 4-10cm is intensely brecciated and irregularly veined with the development of lenticular "pods" or "lenses" of coarsely crystalline and vuggy white calcite (Plate 8). In the lower third of the limestone bed, abundant sub-vertical veins of calcite are also developed, varying from thicker (3-5mm), rather irregular and impersistent vuggy veins to more continuous fine (less than 1mm), straight fractures. Both coarse and fine veins carry small amounts of sulphide minerals and sticky honey-brown hydrocarbon seeps from vuggy cavities. Small globules and botryoidal masses up to 5mm across of glassy, brittle bitumen are also seen in the coarser veins.

The limestone rests on finely laminated (0.5-3mm thick laminae) organic-rich, calcareous siltstone. Carbonaceous laminae are apparent on the exposed bedding plane and significant γ -activity was registered from the surface using a field ratemeter. No samples of this siltstone have been obtained yet for study but further investigation is planned. The limestone is overlain by a highly weathered, regolith of decalcified and gleyed siltstone or very fine sandstone in which the very finely laminated (1-2mm thick laminae) sedimentary structure is well preserved. Samples of this regolith and the brown earth soil profile above have been collected and analysed geochemically but petrographic analyses of this material have not been included in this phase of the study. The limestone represents Facies "A" of Donovan (1980) and the enclosing siltstones are provisionally considered as Facies "B".

Although direct evidence of faulting was not immediately obvious in PIT 1, well-developed slickensided surfaces within the basal brecciated zone indicate shearing of the limestone parallel to bedding. Tectonic movements parallel or sub-parallel to bedding are common features throughout the Caithness Flags (Donovan et al, 1974) and are considered to relate to low-angle thrust movements from the southeast, usually followed by northeast-southwest compression. The thinly-bedded organic-rich laminites (frequently fish-beds) are the usual locations of such bedding-plane movements (Donovan et al, 1974) which are manifested by zones of crushed and slickensided rock cutting vertical or subvertical joints.

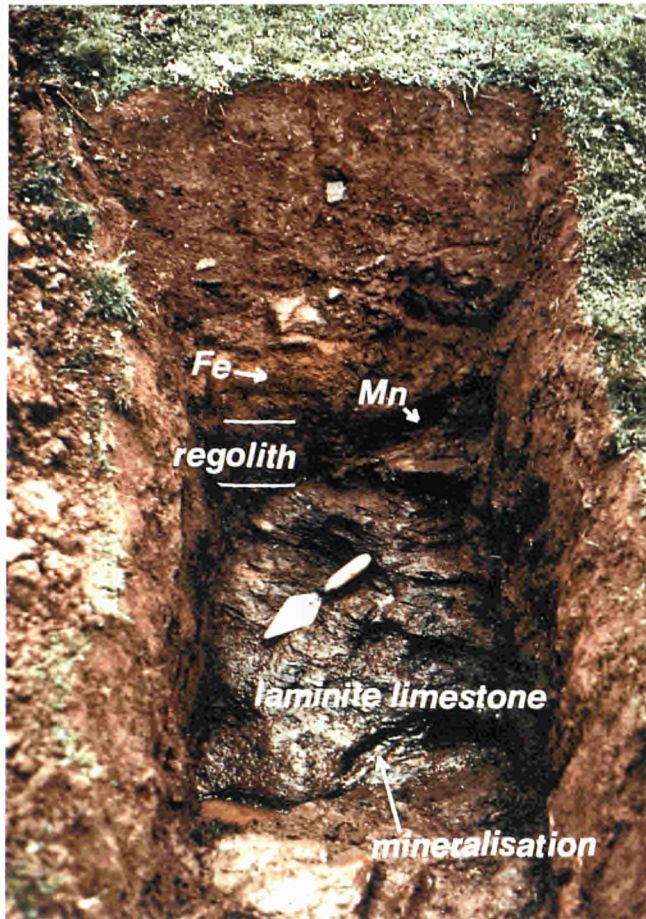


PLATE 7 Photograph of soil section in PIT 1 showing limestone laminite at base of pit. Note zones of Mn and Fe accumulation and staining towards base of soil profile and seepage of water at base of pit.

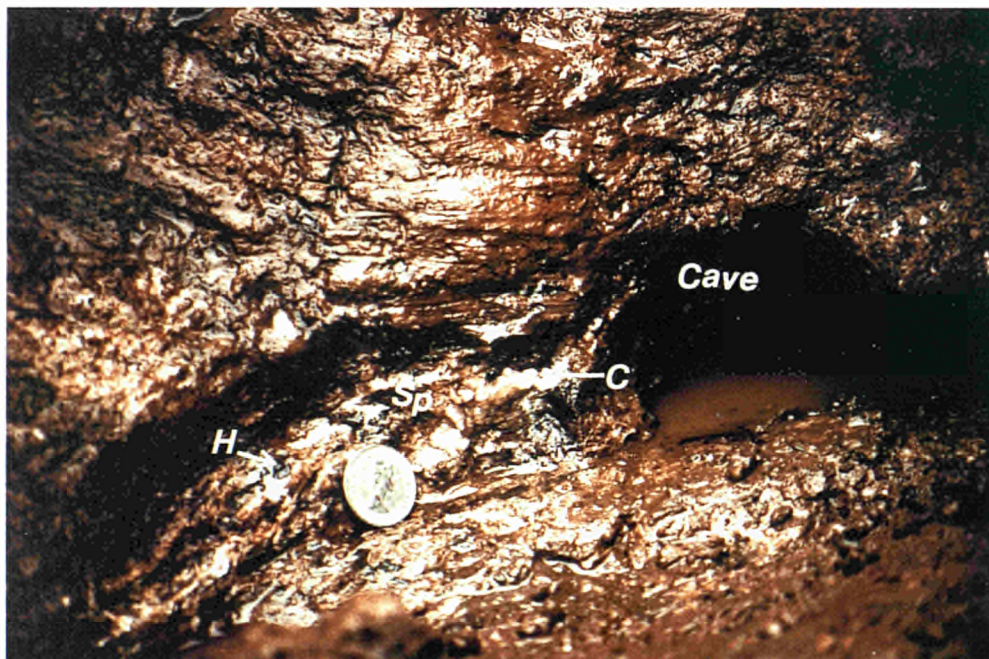


PLATE 8. Detail of base of laminated limestone (PIT1) showing reddish spherulites (Sp) and hydrocarbon globules (H) associated with calcite veins (C) in brecciated rock. Local small-scale cavernous dissolution of the limestone is apparent at its base.

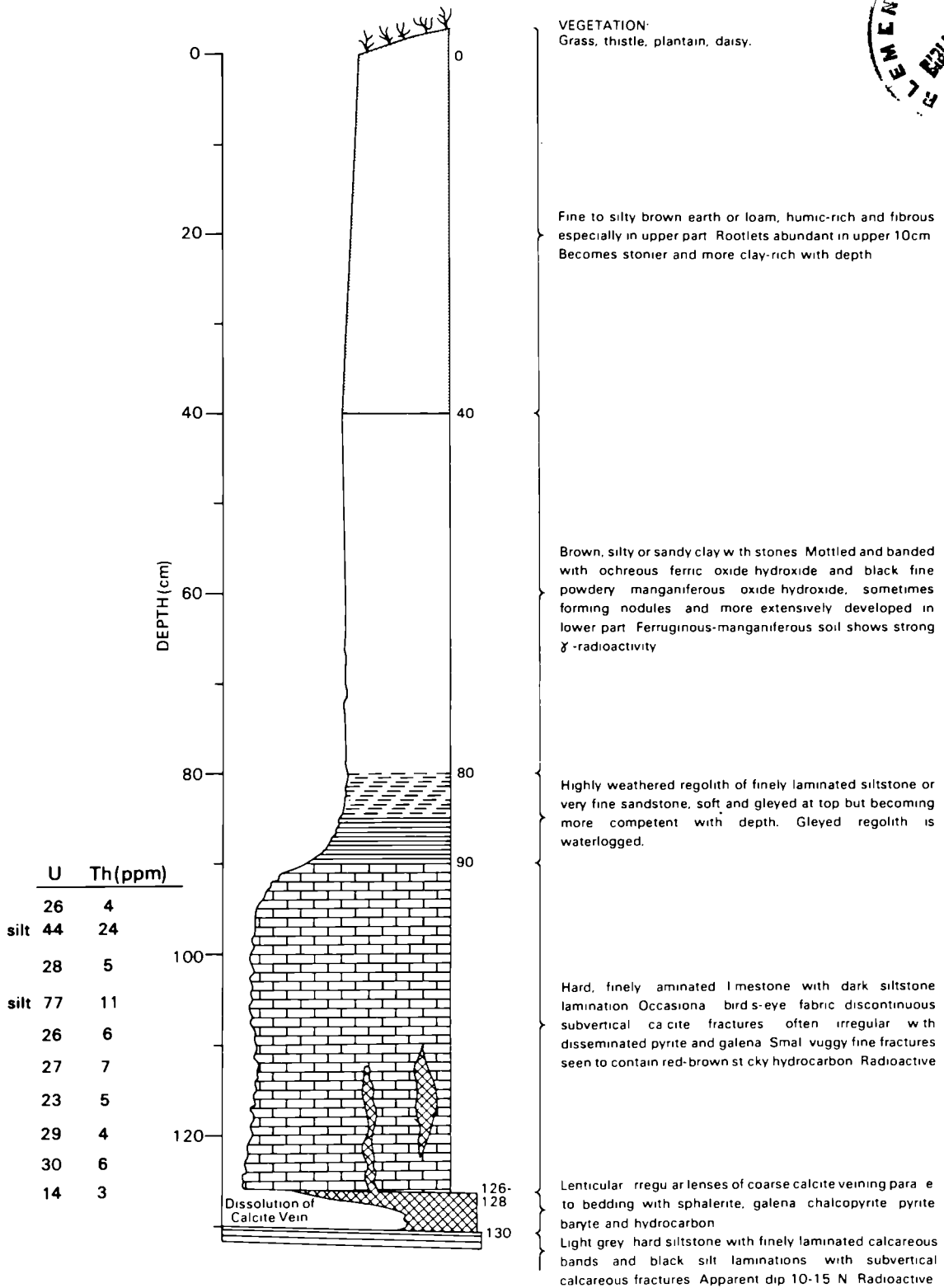


Figure 2: Schematic profile of PIT 1, showing analytical data for uranium and thorium.

Following the conclusions of Gallagher *et al* (1971), evaluation of the source-term has so far concentrated on the examination of the complex mineralogy and petrology of the limestone and its associated vein mineralisation. However, in view of the results contained in this report, this appraisal is being extended to include the siltstones immediately adjacent to the limestone.

3.2.2.2 Sedimentary Petrography

The limestone is finely-laminated, especially in the upper half. It comprises alternations of thin (0.2-0.5mm) bands of recrystallised micrite (microsparrite) with minor scattered silt grains, overlain by very fine (less than 0.1mm) lamellae of dark, organic-rich silty clay which in turn is overlain by lamellae (0.1-0.4mm thick) of coarser siltstone or fine sandstone (Plates 9, 10 & 11). The clastic component is similar to the background flagstones described previously except that dolomite and calcite clasts are notably absent. The organic-rich laminae are often superimposed on siltstone lamellae and are usually represented by fine laminae of pyrite-rich silt or silty clay (Plate 13). The authigenic pyrite is largely present as disseminated, very fine (0.1-1 μ m) octahedra and sometimes as framboidal aggregates. The coarser siltstone is less pyritic.

The "cleaner" siltstone and fine sandstone laminae show extensive development of authigenic quartz and feldspar (both K-feldspar and albite) overgrowths producing well-developed euhedral forms and cementing the laminae (Plate 14). Lack of compaction and deformation of detrital micas indicates that cementation occurred prior to any significant burial. More argillaceous laminae are less cemented and display compactional deformation, as in the flagstones described earlier. However, the earliest diagenetic feature appears to be the pyrite which is often found trapped on the surface of detrital grains beneath later quartz or feldspar overgrowths (Plate 15), closely associated with contemporaneous fine authigenic anatase and apatite (Plate 16). Detrital apatite grains are ubiquitously overgrown by small (2-10 μ m) perfect euhedral authigenic apatite crystals, trapping pyrite, anatase, Y-Dy-Heavy REE-phosphate and U-rich phosphate (?) or silicate (?) on the surface of the detrital core (Plate 17).

The carbonate component of the limestone is extremely complex and multiple generations of both authigenic and vein carbonates are apparent from BSEM and CL analysis. The finely recrystallised micrite (microsparrite) of the carbonate bands (hereafter referred to as C1) luminesces with a dull to moderate orange-yellow CL (Plate 11). In the upper parts of the limestone this microsparrite appears to be relatively homogenous. Authigenic overgrowths of quartz and K-feldspar are enclosed and partly replaced by the microsparrite (Plate 14)

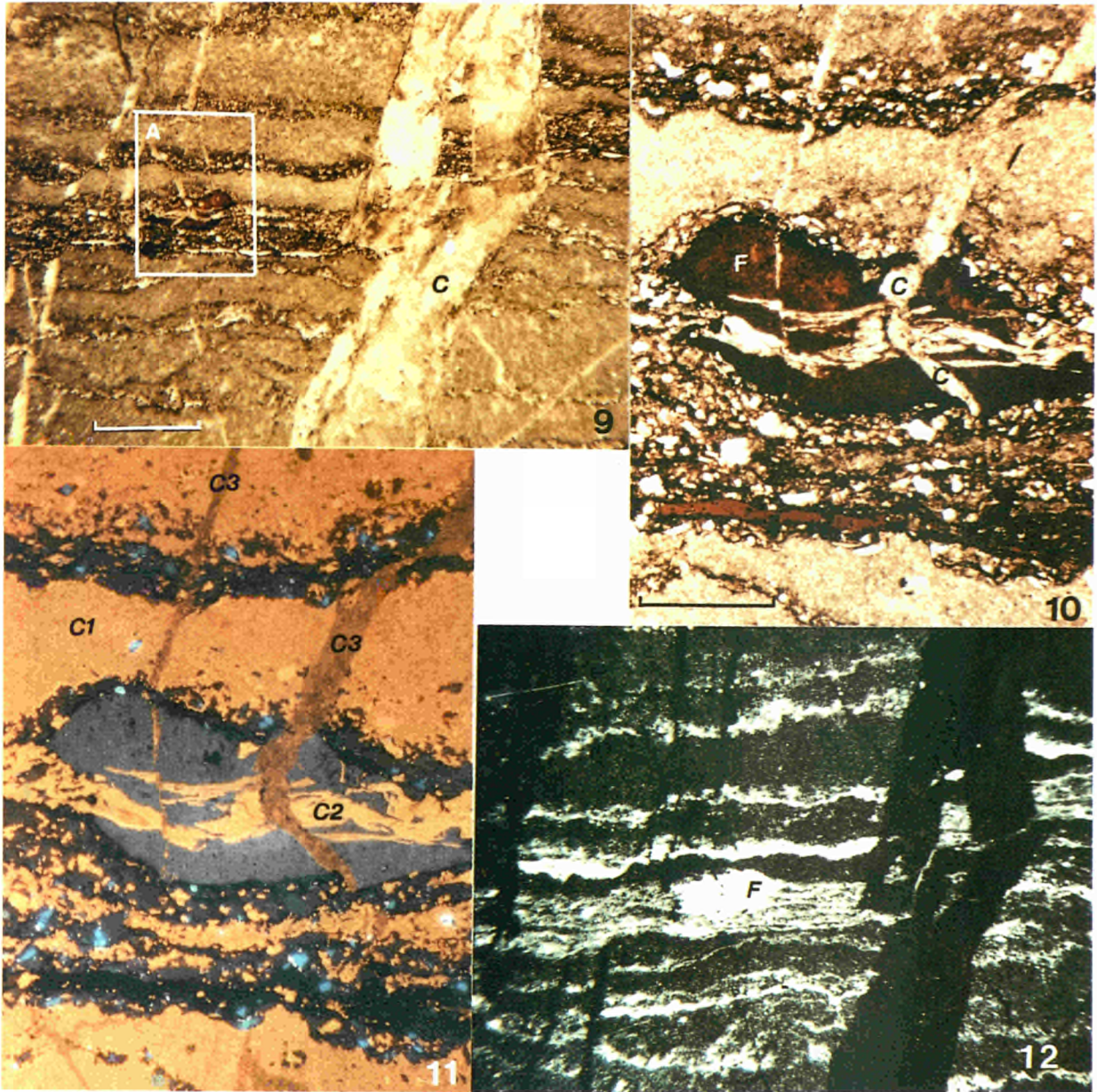


PLATE 9. Typical laminated limestone with interbanded carbonate (micrite/microsparrite) and darker thin organic-silt laminae, both cross-cut by subvertical calcite veins (C). Scale bar: 2mm (plane transmitted light)

PLATE 10. Detail of area "A" in Plate 9 showing brecciated colophane fossil fish fragment (F) within silt lamination. Fossil fragment is veined by calcite (C). Silt laminae show graded bedding, fining upwards and resting on a dark, organic-rich base. Scale bar: 0.50mm (plane transmitted light)

PLATE 11. CL photomicrograph of Plate 10 showing relationships of multiple generations of calcite veining (C2 & C3) to micrite/microsparrite calcite (C1). Note C2 occurs as cement in silt laminae and is cross-cut by later C3 veins.

PLATE 12. Fission track print of Plate 9 showing different concentrations of uranium in the various lithologies. High intensity of tracks seen associated with fossil fish fragment (F). Note fission track prints have been photographed with dark field illumination. Fission tracks show white.

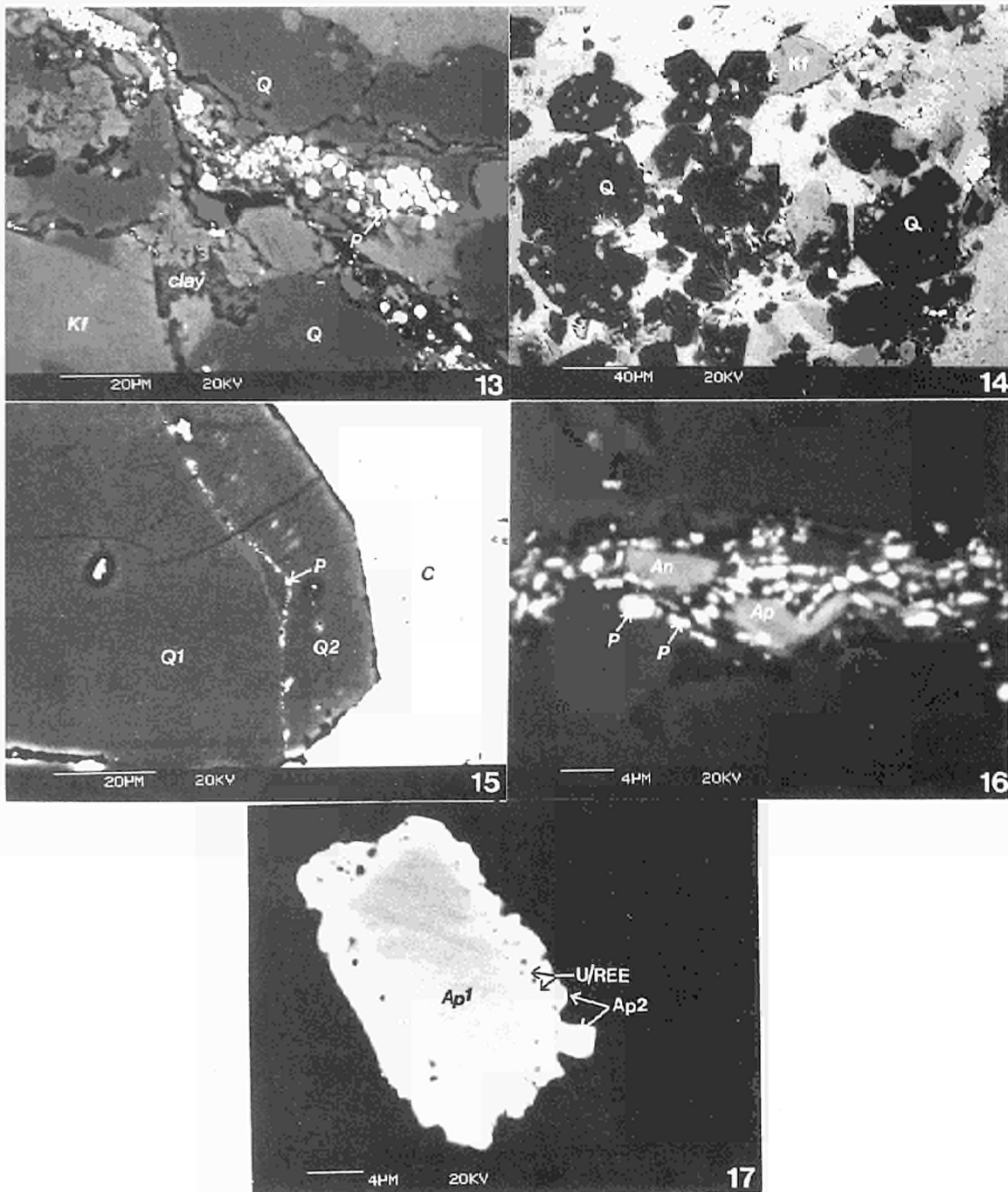


PLATE 13. BSEM photomicrograph showing concentration of early diagenetic finely disseminated and framboidal pyrite (P) concentrated in organic-rich clay laminae in quartz (Q) - K-feldspar (Kf) silt laminae of laminated limestone.

PLATE 14. BSEM photomicrograph of "cleaner" clay-free siltstone laminae in limestone. Note extensive authigenic overgrowths producing well developed euhedral crystal faces on detrital quartz (Q) and K-feldspar (Kf). Microsparrite calcite encloses and corrodes overgrowths.

PLATE 15. BSEM photomicrograph showing very early fine-grained diagenetic pyrite trapped on surface of detrital quartz grain (Q1) beneath later authigenic quartz overgrowth (Q2). Overgrowth enclosed in calcite cement (C)

PLATE 16. BSEM photomicrograph of organic-rich silt/clay lamination containing fine grained pyrite (P) associated with authigenic apatite (Ap) and anatase (An).

PLATE 17. BSEM photomicrograph of authigenic apatite overgrowth (Ap2) on detrital apatite grain (Ap1). Note presence of tiny bright inclusions of U-rich (?uraninite) and Y, Dy, heavy REE-phosphate phases (U/REE) trapped on surface of detrital grain, beneath later overgrowth.

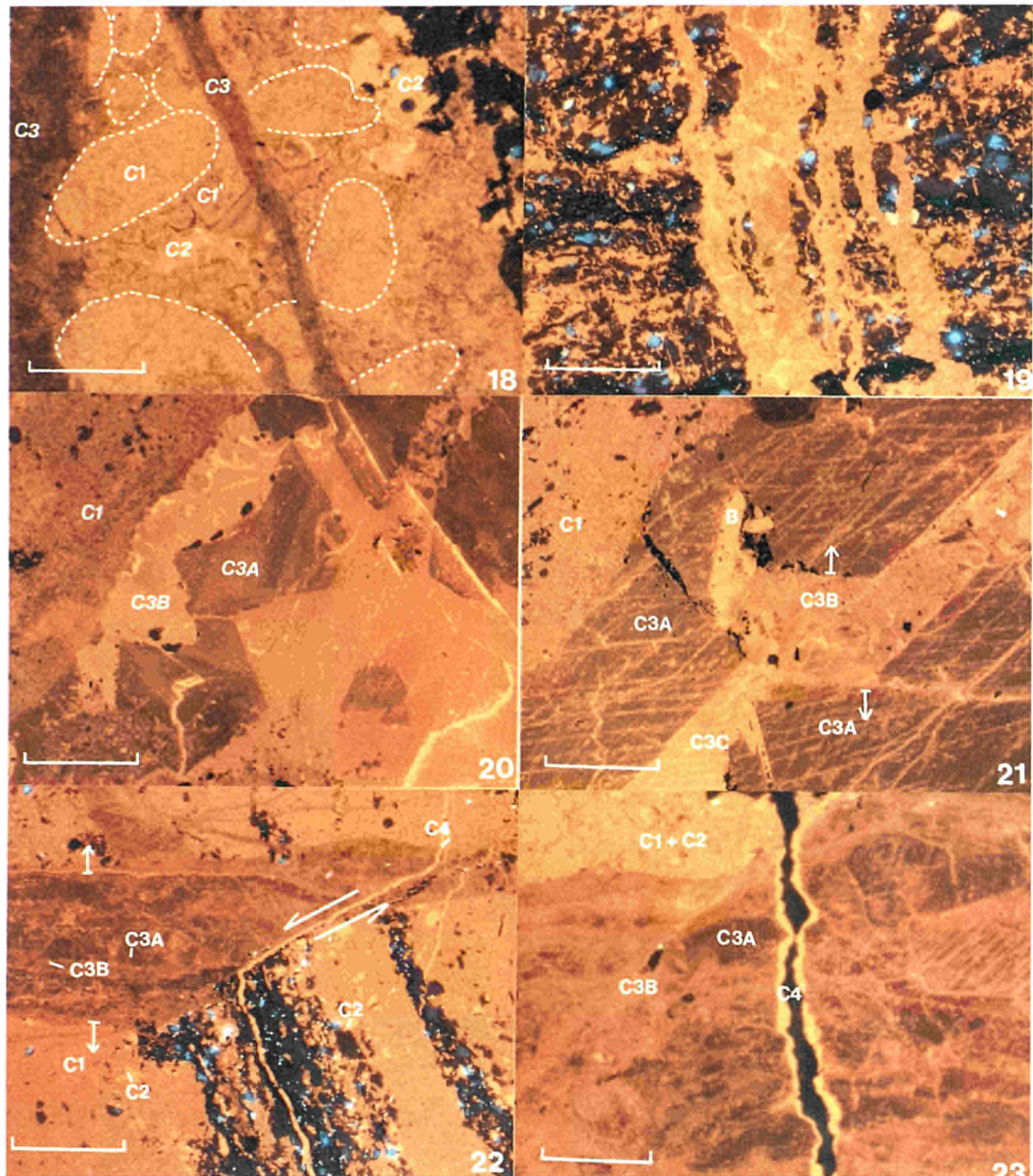
indicating that recrystallisation of the micrite post-dates quartz and feldspar overgrowth.

In the lower part of the limestone bed the micrite laminations are very inhomogenous and must have possessed considerable original or early diagenetic porosity in the form of irregular fissures, fractures and vugs (Plate 18). These features are lined by idiomorphic finely-zoned calcite which has similar CL properties to C1 and can therefore be considered as probably of a similar generation. CL also reveals the presence of small micritic nodules or clasts in the carbonate bands, and the locally extensive development and replacement of siltstone lamellae by both structureless and nodular micrite. A very early origin for the fissures is indicated by the presence of small amounts of geopetal silt infill. The association of nodular micrite and irregular fissuring filled by early diagenetic carbonate described above closely resembles the incipient development of calcretes described from elsewhere in the Orcadian Basin (Parnell, 1983). Alternatively, these pelloidal carbonates may represent early-cemented "oolitic" basin margin sediments.

3.2.2.3 Calcite veining

The vugs and irregular fractures in the limestone are filled by a later bright yellow luminescent (more Mn-bearing) poikilotopic calcite (C2) (Plate 18) which also fills displacive vertical, subvertical and horizontal fractures (Plates 11 & 19) and occurs as a cement in the siltstone lamellae. The CL properties of C2 are identical to the cement in the flagstones (Section 3.2.1) and it may extensively replace detrital grains in the siltstone lamellae, particularly in the lower part of the limestone (Plate 19).

The C2 veins are cut by displacive veins of dull-luminescent ferroan calcite, C3 (Plates 11 & 18). These veins are extremely complex and form a vuggy, repeatedly brecciated fabric with sharp, non-replacive walls (Plate 20). The breccia complex is particularly well-developed in the lower part of the limestone where up to three generations of brecciation and calcite mineralisation can be discerned by BSEM and CL observation (Plate 21). The earliest generation of breccia vein calcite (C3A) is seen as very dull-luminescent (brownish-yellow), coarse idiomorphic spar growing in from fracture walls (Plates 20 & 21). This in turn has been intensely brecciated by fracture movement and the resultant vein breccia is mineralised by slightly brighter, brown-yellow luminescent calcite, C3B (Plates 20 & 21). Sub-vertical veins often "pinch-and-swell" as a result of longitudinal displacive slip-shearing during fracture opening (Plate 22). In these veins C3A is brecciated along shears parallel to the fracture. In the basal breccia zone, but much less commonly higher up the limestone, C3B itself is brecciated and mineralised by a later brighter orange-yellow luminescent low-ferroan calcite, C3C (Plate 21).



- PLATE 18. CL photomicrograph of lower part of laminated limestone bed showing peloidal micritic calcite (C1) cemented by zoned calcite (C11) of similar luminescence lining early diagenetic vuggy fissures cutting laminae. Later brightly luminescent C2 calcite fills remaining vuggy porosity and in turn, is cut by later dull luminescent C3 calcite veins. Scale bar: 0.25mm.
- PLATE 19. CL photomicrograph showing brightly luminescent C2 vein calcite cutting and partly replacing laminated limestone. Scale bar: 0.5mm.
- PLATE 20. CL photomicrograph displaying complex nature of breccia calcite veining at base of laminated limestone. Note "dog-tooth" calcite of initial C3A calcite originally lining limestone wall-rock (C1 calcite) has been brecciated and invaded by subsequent brighter luminescent C3B calcite. Scale bar: 0.5mm.
- PLATE 21. CL photomicrograph of C3 breccia vein calcite showing initial vein infill by dull C3A calcite on wall-rock of micrite/microsparrite (C1). C3A vein has been refractured and pulled apart (as indicated) and subsequently mineralised by progressively more luminescent C3B and C3C calcites. Note lath-like pseudomorph after baryte (B) replaced by bright C3C calcite. Scale bar: 0.5mm.
- PLATE 22. CL photomicrograph of subvertical C3 calcite breccia vein showing slip-shear opening of vein and subsequent multi-generation calcite mineralisation (C3A, C3B). Note very bright luminescent C4 calcite filling fractures cutting and/or following walls of earlier C3 calcite veins. Scale bar: 0.5mm.
- PLATE 23. CL photomicrograph showing detail of very late brightly luminescent C4 calcite mineralisation lining open and fractures cutting C3 calcite veins. Scale bar: 0.25mm.

A further generation of calcite (C4) occurs in very fine veinlets of very brightly luminescent calcite sub-parallel to bedding, or along the walls of earlier calcite veins. These late veinlets cut across C3 structures (Plate 23) and, although sometimes similar in luminescence to C3C calcite, are not related specifically to breccia veins. Many of these late structures are irregular cracks and open fractures lined by uncorroded, euhedrally-terminated calcite syntaxially seeded on the earlier calcite substrate (Plate 23).

The sequence of formation of calcite in the limestone and veins can be summarised as follows :-

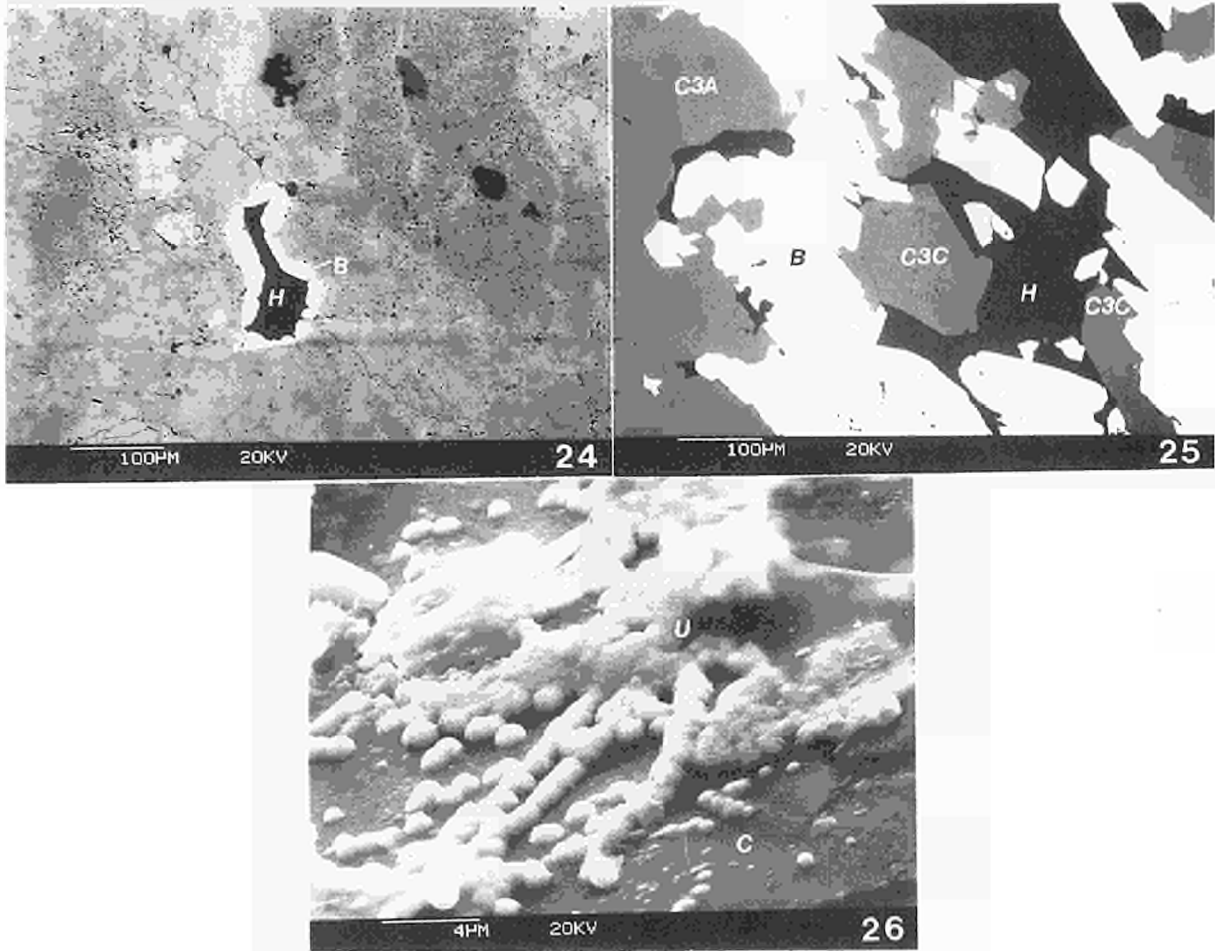
Table 3. Sequence of calcite formation and cathodoluminescence characteristics

CALCITE STAGE	MODE OF OCCURRENCE	CATHODOLUMINESCENCE
C1	Limestone microsparite & vug-lining	Dull to moderate orange-yellow
C2	Later vug- & early fracture-fills; siltstone cement	Bright yellow
C3A	Ferroan, in breccia-vein - first stage	Very dull, brownish-yellow
C3B	Ferroan, brecciating C3A	Brown-yellow; brighter than C3A
C3C	Low-ferroan, brecciating C3B	Orange-yellow to bright yellow; brighter than C3B
C4	Late, cross-cutting fine veinlets	Very bright yellow

3.2.2.4 Other vein minerals

Lath-like crystals of baryte, apparently syngenetic with C3A are common in the basal brecciated veins (Plate 21) and many are replaced to varying degrees by bright C3C calcite or occasionally C3B calcite. Baryte crystals also occur commonly as linings to hydrocarbon-filled vuggy cavities in C3A calcites (Plate 24). The baryte in these vugs is sometimes brecciated and partly replaced by pyrite, chalcopyrite and C3C calcite (Plate 25) but replacement by C3B calcite, as in the veins, was not confirmed.

Sulphide mineralisation, including pyrite and minor chalcopyrite, sphalerite and galena is mainly observed at the boundary between C3C calcite and earlier C3 carbonates, or as wall-rock replacements adjacent to C3 veins. Sulphide mineralisation therefore appears to largely precede C3C mineralisation. Trace amounts of native gold (grains up to 1µm) are also associated, mainly with pyrite.



- PLATE 24. BSEM photomicrograph showing vuggy cavity in coarse breccia calcite vein from base of limestone. Note bright baryte (B) lining vug walls with dark hydrocarbon (H) filling remainder of vug.
- PLATE 25. BSEM photomicrograph of large hydrocarbon-filled vug in breccia calcite vein showing baryte (B) lining wall of vug (C3A calcite). Later C3C calcite has grown on baryte surface partly replacing the earlier sulphate. Later hydrocarbon (H) fills remaining vuggy porosity.
- PLATE 26. SEM photomicrograph showing microbotryoidal uranium-rich phase (U), possibly uraninite or U-carbonate, coating calcite surface (C) of wall of hydrocarbon-filled cavity in C3 calcite veins.

Tiny grains (up to $1\mu\text{m}$) of rare U-rich mineral, probably uraninite, occur at the boundary between C3C and earlier C3 calcites. Similarly, a U-rich mineral occurs as a microbotryoidal coating (possibly uraninite or U-carbonate) on calcite surfaces in hydrocarbon-filled vugs (Plate 26), most of which appear to be in C3A and C3B calcites. Precipitation of the uranium mineral appears to be strongly controlled by the calcite cleavage directions at the vug surface (etched?). No uranium was detectable by EDXA within the hydrocarbon phase, which was found to be a S-rich in all cases from brittle to sticky bitumens.

3.2.2.5 Uranium locations

Fission track prints of polished thin sections of the laminated limestone indicate that uranium is strongly concentrated within the organic-rich silt laminae, is less so in the carbonate bands and is virtually absent from the calcite veins (Plates 9, 12, 27 & 28). This is in good agreement with the whole rock analytical values which show considerably higher contents in the silt-rich samples compared with the samples of "normal" laminated limestone (Figure 2).

Within the organic-silt laminae, fission tracks form a diffuse high background to discrete individual dense track clusters relating to significantly higher uranium concentrations (Plate 29). This background distribution can be related generally to the presence of fine grains of disseminated pyrite (Plates 30, 32 & 33). The very fine nature of the distribution largely precludes identification of a discrete uranium-bearing species using BSEM and electron microprobe analysis, although fine authigenic anatase and apatite have been recognised in close association with the pyrite. This suggests that uranium is perhaps complexed onto pyrite surfaces. However, within the assemblage discrete uranium rich phases (uraninite or U-phosphate or -silicate) were seen, together with HREE, Y-phosphates, trapped beneath authigenic quartz or apatite overgrowths. These phases are syngenetic with early diagenetic pyrite formation and it is possible that these represent the principal mode of occurrence of the uranium within the siltstone lamellae.

The intense clusters of fission tracks in the laminae correspond with a number of detrital components. Moderate track densities are associated with zircons (often metamict, Plate 31), fine anatase pseudomorphs replacing detrital Fe-Ti or ferromagnesian minerals (Plate 32) and detrital apatite with authigenic overgrowths which trap fine U-, Y- and HREE phases. However, the highest uranium contents are associated with subspherical hydrocarbon globules which are common throughout the organic-silt laminae in the size range 50-200 microns (Plates 30 & 33). BSEM indicates that two distinct generations of hydrocarbon are present; an original core containing minute inclusions surrounded by a later inclusion-free rim (Plates 34 & 35). The rims appear to be corrosive towards the host carbonate cement and surrounding detrital components and commonly have associated fine framboidal pyrite around the outer edge of the globule (Plate 36).

Inclusions in the hydrocarbons are mainly anatase with fine overgrowths of U-Ti (possibly brannerite, $(U,Ca)(Ti,Fe)_2O_6$) and U-Ti-Si phases and rarer U-Ti-Ca-Dy-Si phases and fine copper and zinc sulphides (Plates 34, 35, 36 & 37). Small euhedral authigenic anatase crystals 5-10 microns across are observed to grow outwards from hydrocarbons into the matrix. A second discrete group of much rarer hydrocarbon globules is also recognised

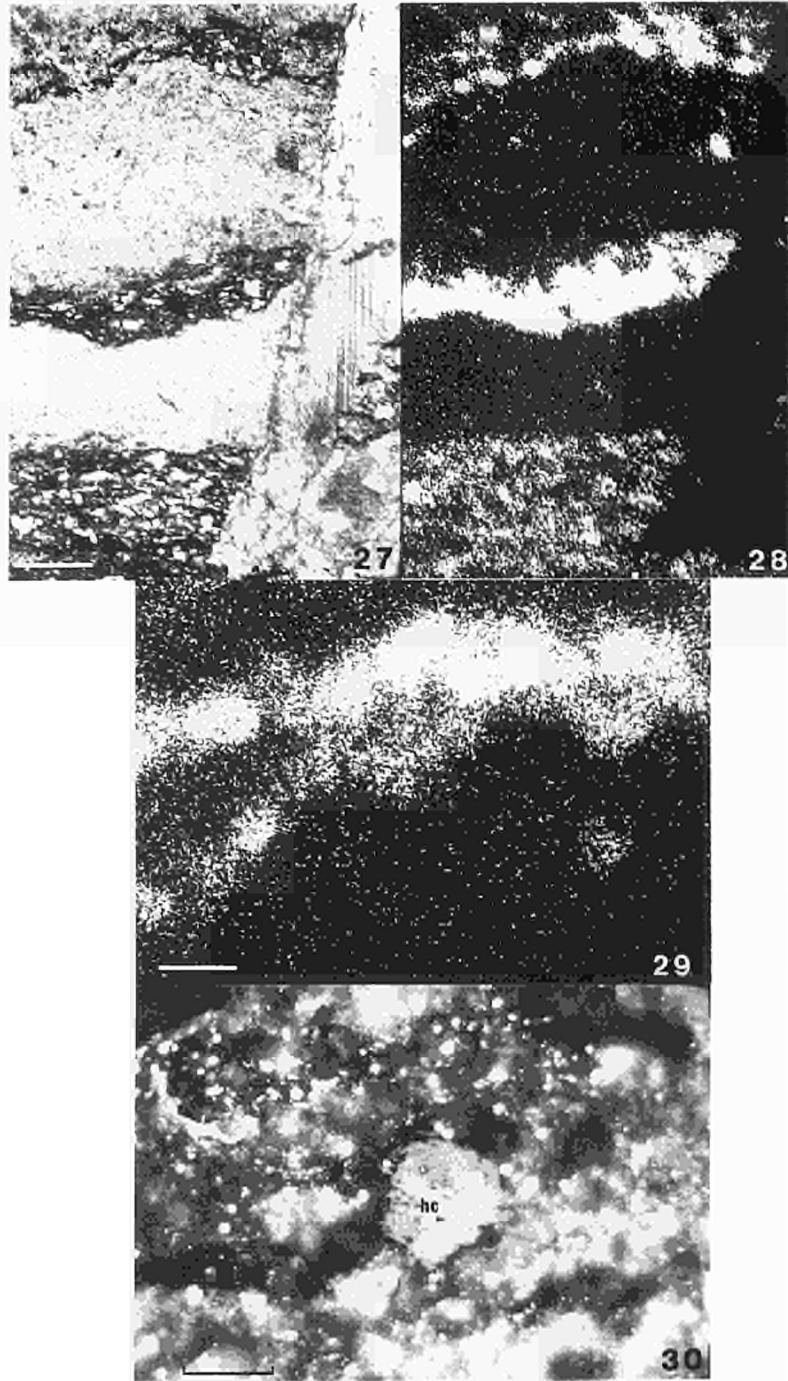


PLATE 27. Laminated limestone with interbedded carbonate bands and organic-silt laminae cut by sub-vertical calcite breccia vein. Scale bar: 0.4mm (plain transmitted light).

PLATE 28. Fission track print of Plate 27 showing high concentration of uranium within organic-silt laminae, less in the carbonate bands, and very low concentration in the calcite vein.

PLATE 29. Fission track print of an organic-silt lamination showing a high background of diffuse tracks amongst discrete individual clusters of high track density. Note the lower concentrations in the surrounding carbonate bands. Scale bar: 0.2mm.

PLATE 30. Organic-silt lamination containing fine disseminated pyrite (bright) and a discrete hydrocarbon globule (hc). Scale bar: 0.1mm (plain reflected light, oil immersion)

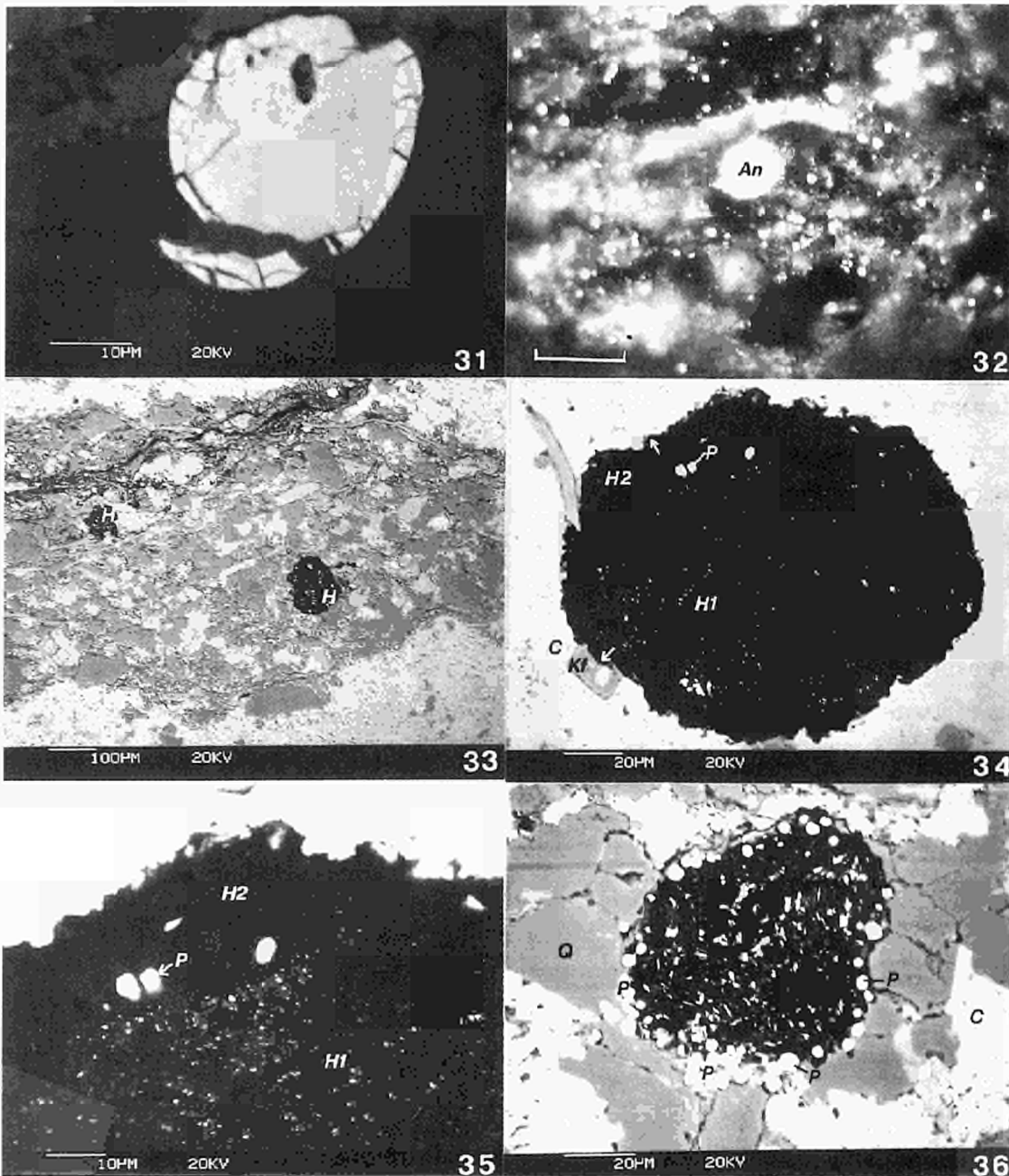
in which the uranium is located in Th-U-silicate phases (Plate 38). Although they may also contain calcium, it appears that thorium and titanium are mutually exclusive (at EDXA detection levels) in individual inclusions and mixed assemblages of discrete Ti-U(Si) and ThUSi inclusions do not occur in the same globule.

Many hydrocarbon cores display an inclusion pattern that resembles a cell-like structure consisting of a network of interconnected individual "cells" each 2-20 microns across (Plate 39). This cellular morphology strongly suggests a biological origin for the mineralised structure within the hydrocarbon. Larger clusters of fission tracks are also associated with lenticular bodies comprising collophanic microcrystalline Ca-phosphate representing fragments of exoskeletons of bony fishes (Plates 10 & 11). Towards the margins of the lenticle the material is less distinctly crystalline and optically more reflective, resembling hydrocarbon. Although the uranium-bearing phases are too small to resolve by SEM, fission tracks are clearly concentrated around such margins and along fractures and cavity surfaces. No discrete hydrocarbon was seen by BSEM to be associated with this material but the collophanic structure appeared to be "degraded". It may be that surface complexing of higher levels of uranium onto the degraded collophane has occurred.

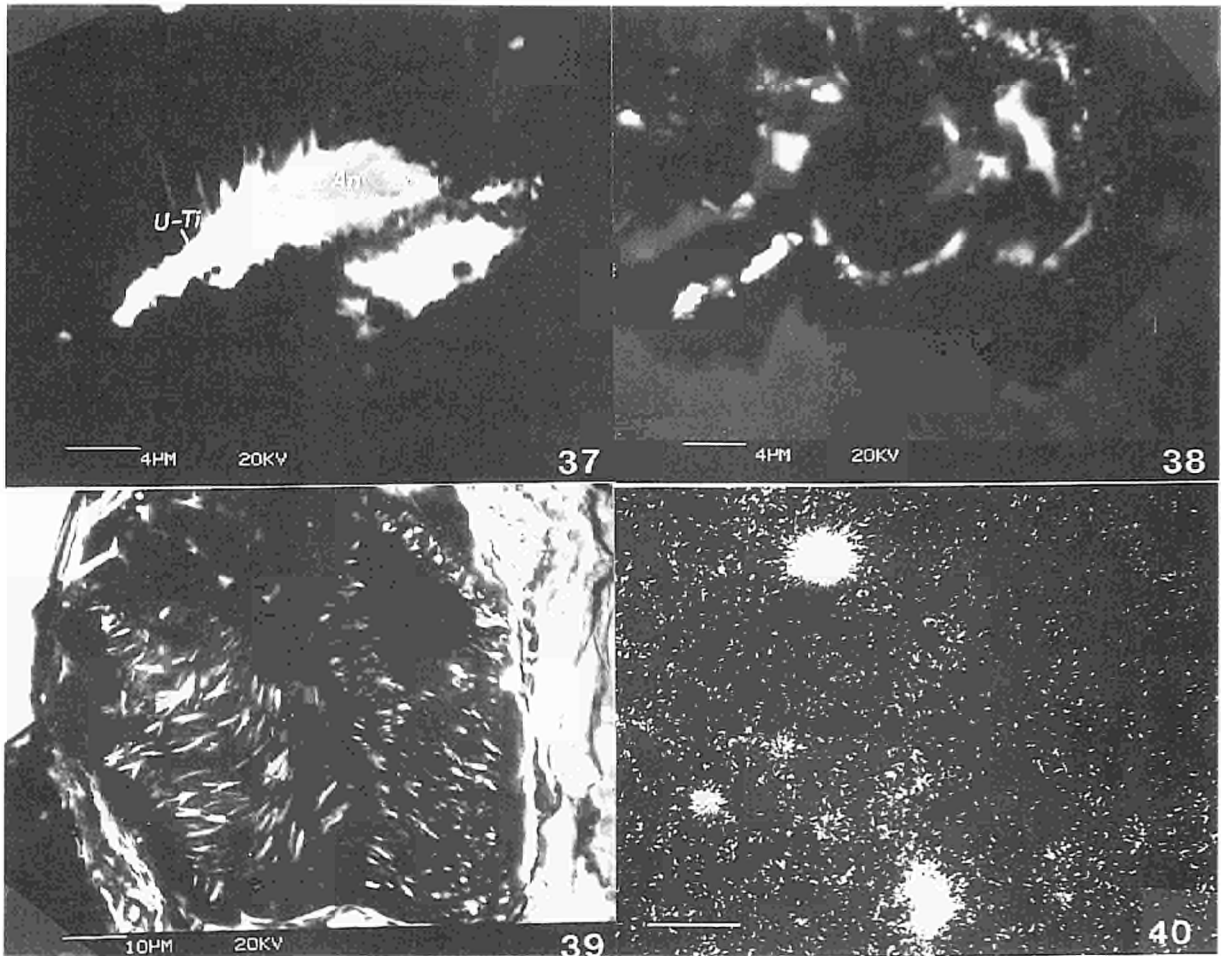
The carbonate bands in the laminated limestone show a more uniform distribution of fission tracks, though of appreciably lower density than in the organic-silt laminae. Only occasional dense clusters correspond to isolated detrital grains (Plates 27, 28 & 40). The dispersed uranium most likely resides within the carbonate lattice or in phases too fine grained and disseminated to be resolvable by SEM.

The calcite veins generally contain very few fission tracks indicating that uranium has remained immobile during most of the veining events. Exceptions to this relate to minute (<1 μ m) discrete grains of a uranium rich mineral (possibly uraninite) and to microbotryoidal coatings along calcite cleavages (section 3.2.2.4). This uranium is associated with a period of sulphide mineralisation immediately prior to C3C vein generation (section 3.2.2.2) but the remobilisation appears to be relatively minor in terms of the total uranium content of the limestone. Fission track prints made under higher neutron fluences show that uranium occurs in very low levels uniformly distributed in the more luminescent, low-Fe C3B and C3C calcite generations but is absent from the C3A breccia carbonate. Fission track analysis and BSEM-EDXA both indicate the absence of either intrinsic uranium or discrete uranium mineral inclusions within the vein hydrocarbons.

Late uranium mobilisation is indicated by a series of linear fission track clusters associated with thin cross-cutting fractures cutting C3 breccia calcite veins and along contacts between



- PLATE 31. BSEM photomicrograph showing metamict zircon from organic-silt laminae. Metamict, hydrated (duller) core has expanded and disrupted the non-metamict (presumably non-radioactive) rim of the zircon grain.
- PLATE 32. Organic-silt lamination containing fine disseminated framboidal pyrite and a large authigenic anatase grain (An). Scale bar: 0.1mm (plain reflected light, oil immersion).
- PLATE 33. BSEM photomicrograph showing globular hydrocarbon particles (H) in silt lamination. Hydrocarbons contain bright U-Ti -rich inclusions.
- PLATE 34. BSEM photomicrograph showing detail of hydrocarbon globules in calcite cemented (C) silt lamination. Note two "generations" of hydrocarbon: core of globule containing minute bright inclusions of a U-Ti mineral (H1); and an inclusion-free outer rim (H2) displaying a corrosive behaviour towards calcite (C) and K-feldspar (Kf) of the host siltstone. Fine pyrite (P) seen at boundary of H1.
- PLATE 35. Detail of Plate 34 showing two phases of hydrocarbon with pyrite associated with boundary of earlier inclusion-rich hydrocarbon core.
- PLATE 36. BSEM photomicrograph of globular hydrocarbon with abundant fine bright inclusions of fibrous U-Ti-rich mineral. Framboidal pyrite (P) is abundantly developed around the borders of the hydrocarbon globule. Note close-packed relationship of associated detrital quartz (Q) cemented by calcite (C).



- PLATE 37. BSEM photomicrograph showing detail of inclusions in hydrocarbon globules. Fibrous bright U-Ti mineral, possibly brannerite (U-Ti) can be seen replacing a core of anatase (An).
- PLATE 38. BSEM photomicrograph of rare Th-inclusion bearing hydrocarbon globules. Bright inclusions are Th-U-silicate associated with duller calcite material.
- PLATE 39. BSEM photomicrograph of fibrous U-Ti-Ca-Dy bearing inclusions in hydrocarbon mimicking probable former cellular morphology of hydrocarbon particle.
- PLATE 40. Fission track print of a carbonate band containing occasional discrete dense track clusters caused by detrital grains within an area of relatively homogenous lower track density. Scale bar: 0.2mm.

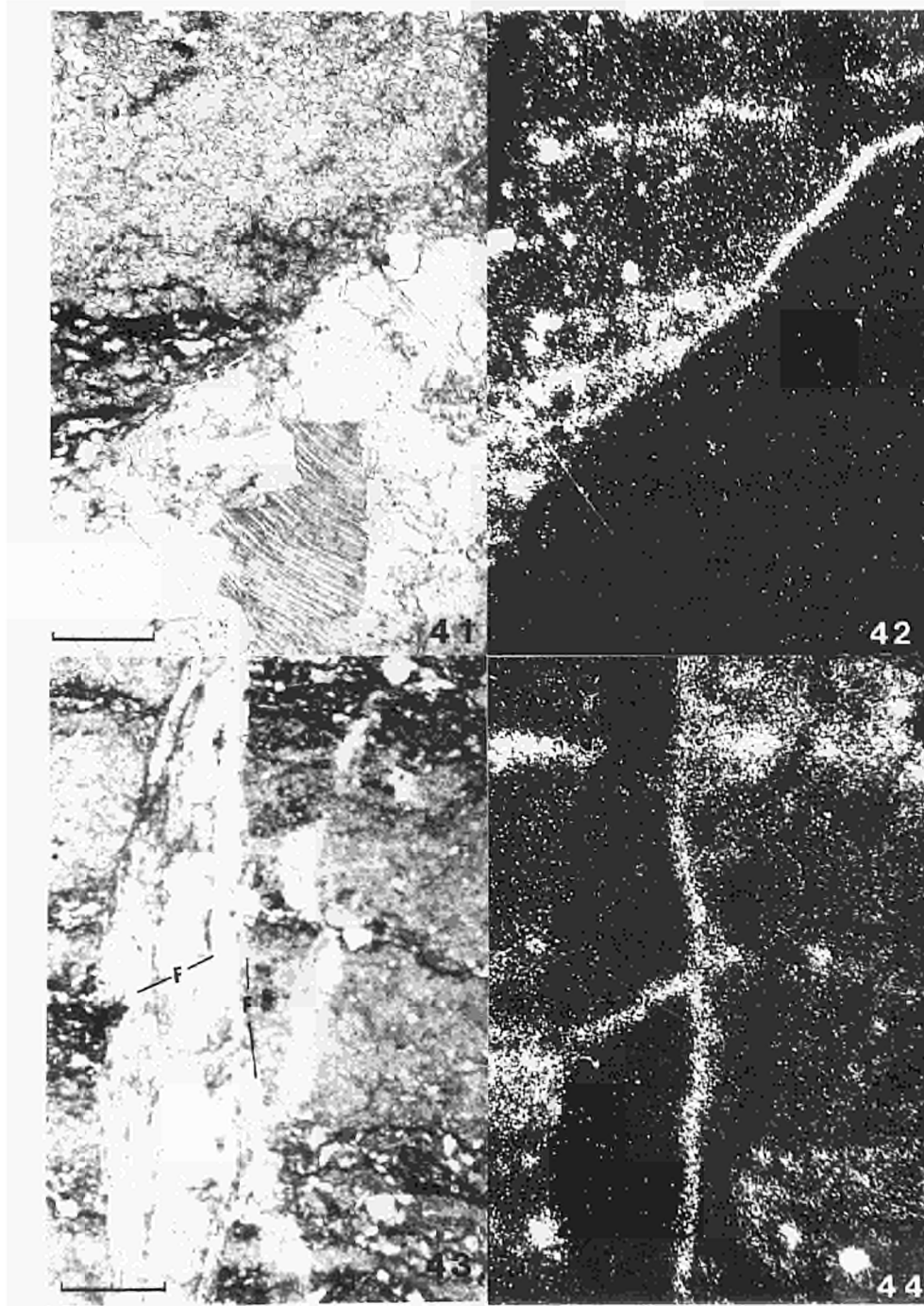


PLATE 41. Details of laminated limestone cross-cut by C3 calcite vein with late microfracture developed along the vein/wall-rock junction (F). Scale bar: 0.4mm (plain transmitted light).

PLATE 42. Fission track print of Plate 41 showing linear track distribution related to uranium mobilisation associated with the late fracture.

PLATE 43. Detail of laminated limestone cross-cut by C3 calcite breccia vein causing vertical displacement of host-rock with late microfractures (F). Scale bar: 0.4mm (plain transmitted light).

PLATE 44. Fission track print of Plate 43 showing linear track distribution related to late uranium mobility along the cross-cutting microfractures.

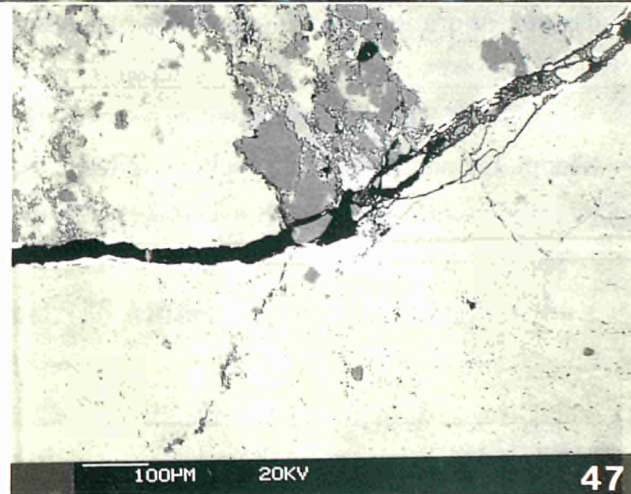
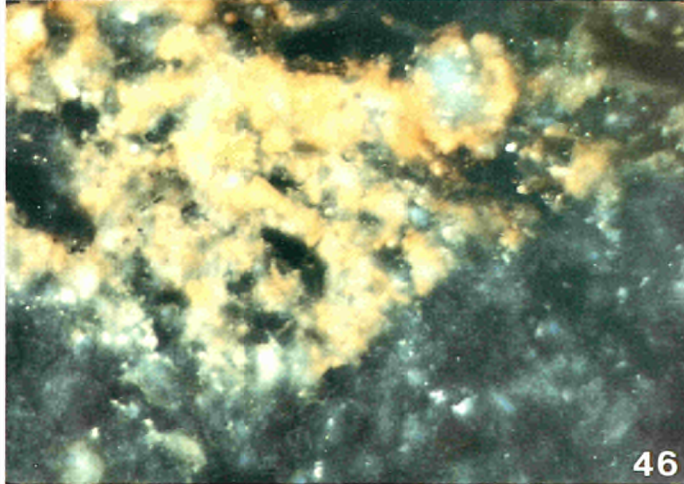
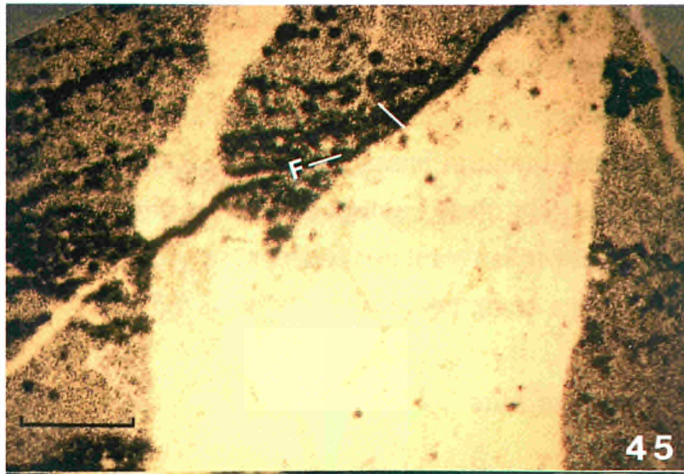


PLATE 45. Fission track print produced under high neutron fluence and photographed under light field illumination (ie. fission tracks are dark) showing uranium mobilisation along a late cross-cutting microfracture (F). The high neutron dose reveals the presence of small concentrations of uranium along grain boundaries in the calcite vein. Scale bar: 0.5mm.

PLATE 46. Yellow goethite developed within an organic-silt lamination by the oxidation of pyrite. Scale bar: 0.1mm (cross-polarised reflected light, oil immersion).

PLATE 47. BSEM photomicrograph of late (open) fracture along borders of C3 calcite vein corresponding to similar fission track concentrations as described in Plate 45. Note presence of fine bright baryte coating the open fracture surface

these calcite veins and limestone wall rock (Plates 41, 42, 43, 44 & 45). The fractures sometimes contain a yellow-brown stain which is associated with the formation of goethite due to oxidation of pyrite in the organic-silt laminae (Plate 46). BSEM and CL indicate that such mobilisation of iron and uranium is associated with baryte (Plate 47) or calcite (Plate 23) coprecipitation along largely open fracture surfaces related to the last phase of calcite veining (C4). This process is probably related to recent or present-day weathering and might be considered as representing a contemporary highly localised source and sink of uranium.

3.2.2.6 Uranium mass balance

Comparison of fission track prints with calibrated uranium standards provides quantitative data on uranium concentrations in specific locations within a sample. Fission track counting of a sample from the top of the laminated limestone indicates an average concentration of 60ppm U for the dispersed uranium in the organic-silt laminae, 25ppm U for the carbonate bands and <1ppm U for the calcite veins. Table 4 relates these data to modal volumes estimated for each lithotype and provides a calculated whole rock mass balance for uranium in the sample. Similar data for a sample from the base of the limestone are also included.

Table 4. Uranium contents determined by fission track counting, modal compositions and derived mass balances for uranium for two samples of the Broubster limestone

LITHOTYPE	LIMESTONE (TOP)			LIMESTONE (BASE)		
	Mode	U content	Whole rock	Mode	U content	Whole rock
Organic-silt laminae	10	60	6	10	50	5
Carbonate bands	75	25	19	65	15	9
Calcite veins	15	<1	—	25	<1	—
			25ppm			14ppm

The table shows that, in both samples, uranium contained in vein calcite is negligible in amount and that the carbonate bands account for significantly more of the whole-rock uranium content than the organic-silt laminae, in spite of the lower intrinsic content in this lithotype. The calculations exclude the dense track clusters related to inorganic detritals and the hydrocarbons. However, the close correspondence in Fig 2 between the calculated whole rock contents (25 & 14 ppm) and the analytical values (26 & 14 ppm) strongly suggests (even allowing for errors in the method) that these phases contribute very little to the overall uranium budget in the laminated limestone.

In comparing the data for the two samples it is to be noted that the contribution from carbonate bands is significantly lower in the sample from the base of the limestone whereas the organic-silt component remains relatively uniform. This appears to correspond with the petrographic evidence of early (pre-C1) diagenetic development of fissures and vuggy porosity related to possible calcrete formation or early diagenetic carbonate "reworking" (section 3.2.2.2) and indicates uranium removal due to carbonate remobilisation at a very early stage.

4. DISCUSSION

4.1 GENERAL

This investigation has revealed a complex history of uranium deposition and redistribution during a sequence of distinct geological events. Uranium mobility can be considered in relation to its origin within the palaeoenvironment of the deposition of the lacustrine sediments of the Orcadian lake, followed by mechanisms of fixation and concentration in the sediments and subsequent diagenetic and tectonic remobilisation and redistribution. Finally, the cumulative effects of these processes in determining the various ultimate host phases of uranium can be assessed with reference to leachability in the present-day weathering regime. A summary of the relationships between the diagenetic processes and uranium mineralisation or enrichment is given in Table 5.

4.2 URANIUM ORIGIN AND THE PALAEOENVIRONMENT

4.2.1 The Lacustrine Model

The deposition of these sediments is envisaged to have taken place in an arid tropical lacustrine sedimentary environment (Donovan, 1975; 1978; 1980; Donovan *et al*, 1973; Mykura, 1983). The upper part of the uraniferous limestone bed encountered at Broubster is largely typical of "Facies A" laminites (Donovan, 1980) in which sedimented triplets of micritic algally-precipitated carbonate, fine organic matter and silty sediment are interpreted as seasonal varves deposited in a relatively deep, thermally stratified permanent lake. These types of sediments are considered to have accumulated in deep, anoxic (reducing) waters and are unlikely to have been subject to desiccation or wave action (Duncan & Hamilton, 1988). However, the studies presented here show that the lower part of the limestone is nodular or pelloidal, fissured and penecontemporaneously calcite-cemented laminated micritic sediment.

These features appear to have been superimposed on an earlier original laminite fabric and strongly resemble those shown by post-depositional calcretes (Parnell, 1983). It is therefore indicated that retreat and shallowing of the Orcadian lake, accompanied by subaerial exposure of the laminites, occurred soon after their deposition. This is consistent with the development of Facies A close to the basin margins (Donovan, 1980), albeit in relatively deep water, where changes in the Orcadian lake level would have a significant effect on the sedimentology and subsequent eodiagenetic processes.

4.2.2 Uranium

Uranium was probably transported from source areas into the Orcadian lake both in solution or colloidal suspension (eg on clays and Fe sesquioxides) and as clastic sediment and the ultimate distribution within the sediments controlled by the processes of fixation, concentration and remobilisation. Much of the uranium mineralisation in the Caithness Flags is thought to depend heavily on early diagenetic processes and, in common with other lacustrine associations, shows a strong correlation with phosphate (Michie & Cooper, 1979). The highest levels recorded in the Caithness Flags (excepting fracture-related occurrences) generally coincide with the postulated basin margin immediately adjacent to basement rocks (Michie & Cooper, 1979; Tweedie, 1981; Michie, pers. comm.). An analogy may be drawn between the situation in the Orcadian Basin and uranium or other metal mineralisation at the capillary fringe (sabkha or playa environment) of present-day arid-region lakes in Australia and Africa (Renfro, 1974; Arakel & McConchie, 1982; Carlisle, 1983; DeDeckker, 1988). In these situations soluble hexavalent uranium produced by oxidative weathering of U-rich basement source rocks is transported in percolating groundwater which discharges at the interface with saline groundwater (Ghyben-Herzberg Interface) at the margin of saline lakes towards the centre of the drainage basin. In modern lakes the discharging groundwaters cause the formation of lake margin calcretes or interact with the algal organic-rich sediments at the lake margin. Uranium may become enriched as a result of these processes in these marginal sediments. Evidence that saline (Na-rich) conditions are likely to have been present in the Orcadian lake is shown by the presence of reported pseudomorphs after trona in "Magadi-type" cherts associated with "Facies A" sediments (Parnell, 1985(a); 1988), extensive development of authigenic albite (noted in this study) and occasional authigenic aegirine (Fortey & Michie, 1978). Nodules of possibly similar "Magadi-type" origin were found at Broubster but have not been characterised so far during this investigation.

Although geochemically anomalous source-rocks are not essential *a priori* for secondary enrichment to occur, given appropriate fixation and concentration processes being operative (c.f. the Yeeleerie uraniferous calcrete of Western Australia), in the present case enriched

basement is present. To the west, granitic members of the Strath Hallidale migmatite complex contain up to 13ppm U and 31ppm Th (Storey & Lintern, 1981) and there is good evidence of remobilisation of uranium from a group of accessory minerals including uraninite, monazite, sphene, zircon and a variety of Nb-Ta-Y-Ti-REE oxides, into more labile sites (Basham, Ball, Beddoe-Stephens & Michie, 1982(b)). To the south, the Helmsdale granite is also enriched in uranium (9ppm mean) and several remobilisation processes are well documented (Tweedie, 1979).

4.3 URANIUM IN THE BROUBSTER LAMINATED LIMESTONE

4.3.1 Deposition and Concentration

For reasons outlined above, the close proximity of the Broubster site to the immediate lake margin during deposition of the limestones is considered important in terms of the primary accumulation of uranium. Fission track studies have shown that levels of up to 25ppm U are present in the micritic carbonate bands. The presumed origin of these as algal induced precipitates suggests that the uranium might be syngenetically derived from solution, although post-depositional (? diagenetic) recrystallisation could have been responsible for some redistribution/reconcentration.

During seasonal algal/cyanobacterial blooms the photosynthesing activity of the organisms would have removed CO_2 from the lacustrine waters thereby raising the pH and inducing the precipitation of CaCO_3 . Concomitant with this process, uranium in solution in the lake waters, probably as a bicarbonate/ U^{6+} complex, would have been destabilised and the uranium would probably have coprecipitated with the CaCO_3 and thereby incorporated in the micritic sediment. High concentration of uranium in the carbonate sediment would have been favoured by the proximity of uranium-rich surface and groundwaters entering the lacustrine environment at the lake margins. The strong correlation of uranium with organic-silt laminae in which the organic components are considered to derive largely from algal material (Donovan, 1978; Marshall et al, 1985) may also result from the direct accumulation of uranium in marginal lake waters. Cyanobacteria (blue-green algae) are known to have a strong affinity for the fixation of uranium (Disnar, 1981) and incorporation and concentration of uranium during seasonal algal blooms is considered likely. This would then become incorporated into the organic-silt laminite, upon death of the algae. Alternatively, uranium-charged oxic groundwaters refluxing through the sediments at the lake margin may have deposited uranium in the organic-rich silty laminae due to the presence of reducing conditions.

Clastic detrital components in the laminated limestone are largely restricted to the organic-silt laminae and include resistate accessory minerals from granitic sources. In terms of the total uranium budget, these are of minor importance and likewise are not considered to represent an appreciable source of labile uranium.

4.3.2 Diagenetic Redistribution

The formation of lake margin calcretes and related soils has been shown to be of considerable importance in the initial accumulation of uranium (Arakel & McConchie, 1982; Carlisle, 1983). This "primary" concentration may then represent a source-term for reworking during subsequent diagenetic processes (Arakel & McConchie, 1982). Erosion of these deposits during "seasonal" storms would rework the uranium which could be transported with terrigenous material (and possibly in solution) in surface and groundwaters into deeper lake environments. At Broubster, it appears that the base of the laminated limestone unit has been affected by processes involving recrystallisation of carbonate and replacement of the original fabric in a manner in keeping with possible incipient calcrete development. Quantitative estimations of relative uranium contents indicates bulk uranium removal although no direct evidence has been found of the destination of the lost uranium. However, calcrete formation would have created an environment in which uranium precipitated in reducing laminites would probably have been subaerially oxidised, complexed with bicarbonate and redistributed into a secondary carbonate or evaporite phase (c.f. Arakel & McConchie, 1982; Carlisle, 1983). A situation involving complex seasonal reworking of uranium within lake margin calcretes, transport and diagenetic fixation in deeper lacustrine facies, followed by further reworking of these sediments by subsequent calcrete development during lake regression could be envisaged as a plausible model.

The earliest diagenetic features preserved in the Broubster limestone are the formation of authigenic framboidal pyrite, fine-grained TiO_2 precipitates or replacements of Fe-Ti-bearing detrital minerals and contemporaneous or slightly later authigenic apatite precipitates or overgrowths. These minerals are closely associated with organic-silt or sandstone laminae in the limestone and also occur in the background sandstones. A significant amount of uranium is spatially associated with the early diagenetic framboidal pyrite which results from the bacterial reduction of iron and sulphur in the anoxic organic-rich silt sediment. Uranium, introduced into the sediment either adsorbed on detrital colloidal material (eg ferric oxides), complexly fixed in decaying algal remains or in solution in groundwater at the lake margin as discussed above, would have been reduced to the insoluble tetravalent species and precipitated or sorbed onto growing sulphide surfaces which represent the reduction sites. The discrete, fine uranium minerals (?uraninite) and REE phosphates seen in association with

apatite, nucleating Ca-phosphate precipitates, and fine grained TiO₂ are also considered to be syngenetic. The presence of early diagenetic, authigenic quartz, albite and K-feldspar indicates that the cleaner silt and sand laminae were relatively uncemented and represented porous and permeable pathways for pore fluids during early diagenesis.

Another potentially significant uranium source in terms of their high uranium concentrations are the common U-rich and, less usually Th-rich, hydrocarbon globules found in the organic-silt laminae. Similar globular hydrocarbons have been described from elsewhere in the Caithness Flags by Parnell (1985(b)). On the basis of their corrosive boundaries, generally spherical shape and lack of organised internal structure, these have previously been interpreted simply as hydrocarbon migrated into the sediment which subsequently absorbed uranium from groundwaters. However, this explanation is inadequate to explain the observations made in the present study.

In many cases the U-rich inclusions within the hydrocarbon globules define a relict internal fabric which, in some cases, resembles cellular structures similar to heavy metal-stained bacterial membranes described from present-day and Eocene sediments associated with uranium-phosphate and sulphide mineralisation (Degens & Venugopalan, 1982; Beveridge et al, 1983). Bacterial and other microbial membranes are known to have an affinity to bind heavy metals such as uranium and this property is utilized in the preparation of electron microscopy specimens (Cole & Popkin, 1981). It is clear that the structures seen within these globular hydrocarbons must also have a biological origin.

The restricted occurrence of these globules to the silty laminae might be taken to indicate that they originated from detrital mineralised organic matter. The cell-size and morphology of the aggregated cellular structure is comparable with coccoid, colonial cyanobacteria (blue-green algae) that construct pustular algal mats in present-day ephemeral and saline lakes (Bauld, 1981). Algal mats are extensively developed at the margins of warm ephemeral and permanent saline lacustrine environments and it is conceivable that they existed at the margins of the Orcadian lake. It is also in this lacustrine zone that sabkha-discharges are most likely to occur (stimulating algal growth) with significant accumulation of metals likely to occur as a result of sulphide reduction beneath the mat surface (DeDekker, 1988) and as described above, cyanobacteria (blue-green algae) have a strong affinity for uranium. This model has also been applied to organic-controlled uranium mineralisation in the Precambrian Witwatersrand Basin of South Africa (Pretorius, 1975). The incorporation of organic fragments into the siltstones might be expected as a result of seasonal storm-scouring of the lake margin, causing erosion of sabkha-mineralised algal mat material and its subsequent transport with terrestrial silt to deeper waters. This is consistent with the sedimentological

model postulated for the Orcadian Basin (Donovan, 1980).

Unfortunately, the detrital origin outlined above fails to account for the corrosive/replacive nature of the globule margins, nor for the excellent uncompacted preservation of the delicate cellular internal structure of the hydrocarbon globules. The cellular structure of organic detritus derived from erosion of algal mats would not be expected to have survived even minor sediment compaction. Therefore the hydrocarbons are unlikely to be detrital organic particles and a post-depositional diagenetic origin is more plausible. One possible explanation is that they represent small-scale hydrocarbon migration and nucleation within the sediment after early lithification, locally replacing the calcite cement and siliciclastic components. Subsequently, this hydrocarbon may have been biodegraded during further diagenesis by bacteria introduced by percolating groundwaters. The bacteria probably sorbed uranium present in the diagenetic porewaters and immobilised it within their cell walls. Basham et al (1989) have described similar uranium biomineralisation in vein hydrocarbons as a result of bacteria using the hydrocarbon as a nutrient source. The rigid framework of the early lithified sediment would have prevented compaction of these delicate mineralised structures. The presence of framboidal pyrite in the outer rim of the hydrocarbon globules is compatible with mineralisation occurring as a result of bacterial sulphide reduction processes. The hydrocarbon globules must represent a much earlier stage of hydrocarbon migration than the non-uraniferous fracture-bound hydrocarbon associated with tectonic movements (section 4.3.3).

A further association of uranium with diagenetically modified clastic material is seen in fossil fish fragments where concentration appears to have been enhanced by degradation of the bone phosphate to more poorly ordered collophanic material. Together with the authigenic phosphates discussed above, this association probably represents the mechanism generally accepted for the phosphate-related mineralisation throughout the Caithness Flags (Michie & Cooper, 1979).

Table 5. Summary of relationships between diagenesis and uranium mineralisation in the Broubster limestone

<u>DIAGENETIC/SEDIMENTARY PROCESS</u>	<u>URANIUM MINERALISATION</u>
1.DEPOSITION:	
i) algal photosynthetic precipitation of micritic CaCO ₃	possible coprecipitation of U with Ca in carbonate from euphotic lake waters (epilimnion)
ii) death of algae and deposition of organic algal remains	possible bioconcentration of U from epilimnion waters within algal cells and accumulation within organic sediment upon algal death
iii) Deposition of detrital sediment	Deposition of minor U-bearing heavy minerals
2.EODIAGENESIS:	
i) Formation of fine grained and framboidal pyrite during microbial sulphide reduction and decomposition of organic matter in reducing organic-rich sediment. Closely accompanied by breakdown of unstable Fe-Ti minerals and replacement by anatase. Precipitation of authigenic apatite.	a) Remobilisation of U from algal organic matter and precipitation of UO ₂ species in close association with pyrite, and/or; b) Reduction of U ⁶⁺ present in oxic groundwaters discharging through the reducing sediments at the lake margin and the precipitation of reduced UO ₂ species in close association with pyrite. c) incorporation of U in anatase d) precipitation of minor discrete U-REE phosphate or incorporation of U in authigenic apatite overgrowths
ii) Precipitation of authigenic quartz and K-feldspar overgrowths with lithification over silt laminae	
iii) Recrystallisation of micritic carbonate to form C1 microsparite and lithification of calcareous sediment	Redistribution of U initially in micritic component into the microsparite (C1) calcite cement

3.MESODIAGENESIS

- i) Burial and compaction
 - ii) Minor formation of liquid hydrocarbon and localised migration into more permeable silt and sand laminae with local corrosion and replacement of siliciclastic and carbonate fabrics
 - iii Biodegradation of hydrocarbon globules Microbial enrichment of U in association with biodegraded hydrocarbon globules
 - iv)Fracturing and precipitation of C2 calcite cements and fracture infills (precise relationship with ii) and iii) above not exactly known but possibly closely associated)
 - v)Repeated fracturing during Late Caledonian and/or Variscan tectonic movements and vein mineralisation by C3 calcites, minor sulphides, baryte and migration of liquid hydrocarbon in fractures. Minor localised remobilisation of U from organic matter and early diagenetic pyrite. Incorporation of very low concentrations of U in C3B and C3A calcite and as very minor discrete U vein minerals
-

4.3.3 Tectonic Remobilisation

Five generations of carbonate cementation and veining subsequent to the early diagenetic processes described above can be discriminated at Broubster. The complex sequence of vein generation generally involved very little interaction with the host laminated limestone and therefore very little uranium remobilisation. However, calcite veining of the C3 generation, which involved brecciation and tectonic disturbance at the base of the limestone unit, was associated with sulphide mineralisation and uranium mobilisation. In this paragenesis, three generations of carbonate mineralisation are associated with movement along bedding plane thrusts. Initial calcite and baryte precipitation was followed by a second generation of calcite which in turn was closely superseded by sulphides, uranium and gold deposition before a third and final episode of calcite precipitation. Hydrocarbon migration occurred after each episode of calcite mineralisation resulting in a range of hydrocarbon species being formed. This complex event possibly involved hydrous fluids associated with a basal shear zone which induced oxidation of the organic-silt laminae assemblage, followed by vein mineral precipitation. It was probably at this stage that the "fault-bounded" mineralised vein, considered originally as the source of the uranium mineralisation, was formed. The variations in hydrocarbons seen in vugs, ranging from sticky liquid to brittle bitumen, might reflect the maturity of the hydrocarbon source at the time of migration. Organic geochemistry

studies of MORS source rocks in the Orcadian Basin indicate that the sediments reached maturity and attained peak hydrocarbon-generating potential during late Devonian or early Carboniferous (Parnell, 1985(d); Marshall et al , 1985). Although hydrocarbons may have been generated by actual thrust movements, it is also likely that the postulated late-Caledonian movements (Donovan, 1974) coincided with the "oil-window" of the sediments. Uranium was probably remobilised from the local sediments (in particular from the organic components that may have been undergoing maturation) during this process.

4.3.4 Supergene Redistribution

Oxidation of the organic-silt laminae by contemporaneous or recent weathering occurs throughout the limestone and is considered to result in the liberation of uranium held in association with diagenetic pyrite. The association of mobilised uranium with goethite, baryte and calcite of the last (C4) generation in open fractures indicates that some uranium is being "fixed" close to source in secondary minerals. These minerals might also be expected to contain other radionuclides (e.g. radium in baryte and calcite). Precipitation of uranium in the young carbonate fractures might be indicative also of the transport of uranium as a bicarbonate complex within the area of the old limestone workings.

4.4 DEFINITION OF THE BROUBSTER SOURCE TERM

Extensive studies have established that uranium is contained in a variety of locations in the laminated limestone and has been subjected to several mobilisation and reprecipitation events. Mass balance studies indicate that the carbonate bands constitute the major source of uranium in quantitative terms but the controlling factor in defining the most significant source is the potential for leaching of uranium from each identified site, irrespective of concentration. Extensive removal of uranium from part of the carbonate occurred at a very early stage in the diagenesis although it appears that this uranium was lost from the local geochemical system. Subsequent mobilisation was caused by oxidative processes acting upon the organic-silt laminae. Although not as significant volumetrically as the carbonate bands, the organic-silt laminae contain higher intrinsic levels of uranium and, due to the presence of fine disseminated pyrite, are more susceptible to oxidative alteration and hence to the leaching of uranium.

Therefore, the main mechanisms of uranium leaching from the laminated limestone are likely to be two-fold :-

1. oxidative weathering of organic-silt laminae by percolating groundwaters (reaction of pyrite (FeS_2) with oxygenated groundwater generating acidic (H_2SO_4) conditions and resulting in : a) the formation of Fe-oxides (goethite); b) dissolution of detrital grains with the release of Ba from feldspar or calcite and its concomittant reprecipitation as baryte (BaSO_4); c) oxidation of U^{4+} to mobile U^{6+} .
2. bulk dissolution of limestone carbonate bands by acidic porewaters related to pyrite oxidation or, more generally, the pervasively acidic groundwaters emanating from the overlying peaty soils.

It appears that these processes have been active at several stages in the past but can be considered to be effective in the post-glacial weathering regime during which the geochemical dispersion pattern in the Broubster Natural Analogue Site developed.

The formation of a mineralised calcite vein at the base of the limestone unit (assigned to the C3 calcite generation event) involved relatively minor uranium remobilisation and is considered not to be significant in terms of a labile source. The Broubster source-term is therefore defined as comprising the entire laminated limestone unit, with contributions being made to the groundwaters from both the dissolving carbonate bands (calcite) and from the release of uranium closely associated with oxidising pyrite in the organic-silt laminae. The lithological and geochemical similarity of the organic-rich, calcareous Facies "B" siltstone below the limestone to these laminae, and the marked contrast to the background lithologies examined, suggests that some attention needs to be given to assessing the possible contribution from that horizon. It is also noted that the overlying highly weathered siltstone (also a possible Facies "B" lithology) shows contents of uranium and thorium comparable to those in the organic-silt laminae. While this in itself may indicate that these elements have not been significantly mobilised by the weathering processes, the possibility of migration throughout the horizon cannot be discounted and should be investigated further. Additional study of the organic-silt laminae and Facies "B" beds is also warranted in respect of analogue modelling of thorium and REE's, as useful comparison may be made between unaltered and highly weathered representatives of similar lithologies. (It is to be noted that the carbonate bands contain very low levels of these elements and therefore do not present a potentially useful source-term for modelling.)

It is significant that the limestone unit at Broubster continues in a northeast direction beneath the site of the present radiometric anomaly, and it seems apparent that, under favourable hydrological conditions, direct vertical migration of uranium could be a major contributory factor to the anomaly in the peat. Further consideration of this must rely upon delineation of the hydrological system above the limestone along its strike length and on establishing the

distribution of glacial till and its capacity for efficient retardation of groundwater movement and dissolved species.

5. CONCLUSIONS

A detailed petrographical and mineralogical study has been made of the laminated limestone unit being considered as the source-term in the Broubster Natural Analogue Site with the following conclusions :

1. On lithological, mineralogical and geochemical grounds, the laminated limestone unit can be considered as a fairly typical member of the Facies "A" association distinguished by Donovan (1980) in the cyclically sedimented MORS Caithness Flagstone succession. It is interbedded above and below with finely laminated organic-rich calcareous siltstone bands, which are considered to belong to Facies "B".
2. A complex genetic history has been established which includes sedimentation, early diagenetic modification and mineral growth, later fracturing and veining, and contemporaneous supergene alteration. These processes have all played varying but integral parts in the origin, fixation, distribution and remobilisation of uranium within the sediment.
3. The bulk uranium content of the limestone unit is significantly enriched (23-30ppm U) compared with the background regional siltstone lithologies (2-7ppm U) although thorium contents are comparable or slightly lower (4-7ppm Th as opposed to 5-8ppm Th). Fine laminae of organic-silt within the limestone show even higher levels of uranium (up to around 60ppm U), apparently in keeping with those in the immediately adjacent siltstone beds. Thorium contents in this lithology range 11-37ppm Th, in marked contrast to the levels in the "average" carbonate-dominated limestone.
4. Detailed study of the location and quantitative distribution of uranium indicates that the carbonate bands in the limestone account for around 80% of the whole rock content. This uranium is held as a fairly uniformly dispersed distribution of around 25ppm U within the carbonate component, most probably contained by crystal lattice substitution. The remaining 20% of the whole rock uranium is concentrated in the organic-silt laminae which account for approximately 10% of the limestone rock volume. Within this lithotype, levels of up to 60ppm U occur as a diffuse association with finely disseminated diagenetic pyrite, apatite and anatase. Very fine, discrete uranium-bearing mineral phases appear to account for much of this uranium, as oxide, silicate or phosphate, at times in combination with REEs. Much

higher levels of uranium occur in association with titanium and silica or with thorium and silica, in hydrocarbon globules which are considered to be of biogenic origin. However these, together with detrital heavy mineral species, contribute only a minor part of the whole rock mass balance for uranium.

5. Uranium, derived from weathering of the provenance areas of the sediments themselves, is considered to have been introduced syngenetically into the sedimentary environment in solution, colloidal suspension and, to a minor extent, as detrital minerals from a predominately granitic source. Seasonal algal life cycles are thought to have been the principal factor in the early fixation of uranium in the sediment, into locations which have been largely stable over considerable time.

Precipitation of the carbonate bands is related to algal growth and photosynthesis and association and accumulation of uranium in this lithology is considered to be contemporaneous with formation or with later diagenetic recrystallisation. Early subaerial diagenetic alteration has resulted in modification in part of the limestone unit, with loss of uranium from the system during calcrite-type recrystallisation of carbonate. Thorium has not been enriched by these processes.

Within the organic-silt laminae, in addition to minor input from detrital heavy minerals, concentration of uranium from lacustrine (epilimnion) waters by living algae and their accumulation within the sediment upon their death, and/or the fixation of uranium within the reducing organic-rich sediment from uranium-charged groundwater during early diagenesis can account for the major part of the uranium. Part of this organically-fixed uranium may be contained within the organic matter itself in a dispersed form and part may have been redistributed diagenetically. Indeed, the main uranium association is in the finely divided diagenetic minerals intimately associated with framboidal pyrite and possibly with the associated fine amorphous organic sediment. Also uranium is associated with early diagenetic hydrocarbon as discrete included minerals.

6. Late or post-diagenetic redistribution of uranium has been of minor extent. Although several successive generations of tectonically-related complex calcite veining have pervasively affected the limestone unit, only one event appears to have involved significant mobilisation of uranium. This was associated with a phase of sulphide mineralisation in which introduction of metals, probably in hydrous fluids, was accompanied by formation of calcite and baryte and the migration and emplacement of liquid hydrocarbons. It seems likely that this event mobilised some uranium into mineralised fractures with reprecipitation in a more labile, accessible form along calcite grain boundaries and on the walls of calcite-lined

vuggy cavities prior to their infilling with migrating hydrocarbons.

7. Recent to present-day supergene weathering processes are effective in mobilising uranium. Oxidation of pyrite in the organic-silt laminae initiates acid leaching from more accessible sites within that lithology while dissolution of calcite in the carbonate bands in percolating acidic groundwaters gives direct release of uranium as the soluble carbonate complex. Uranium minerals present on the walls of vuggy cavities, though probably in a labile form (eg uraninite or uranium carbonates) may be rendered immobile in the present groundwaters, being protected from dissolution by the presence of vug-filling hydrocarbons which themselves have very low solubilities (Smith et al, 1989).

8. In summary, the Broubster laminated limestone is concluded to be a sedimentary unit which presents a fairly persistent horizon of uranium enrichment within the Broubster Natural Analogue Site and, where outcropping in the western part of the site, can be shown to contribute uranium in solution to the present-day groundwater regime. Within the limestone unit, the two principal lithologies contain uranium in different associations, involving different, but related mechanisms for its release. The organic-silt laminae represent around 10% of the source-rock and contain around 20% of the total uranium. Although the bulk of this appears to be contained in very fine grained composite diagenetic minerals (often in association with rare earths and in intimate textural relationships with other, weakly soluble minerals), the close spatial relationship to dispersed diagenetic pyrite results in oxidation and mobilisation concomitant with pyrite oxidation. Acidic solutions generated by this reaction probably play an important role in this respect. Uranium associated with sedimentary carbonate accounts for 80% of the total, contained in around 75% of the limestone. As this appears to be held in the carbonate lattice (or as a sub-crystalline dispersed phase), liberation into solution necessitates total dissolution of the carbonate. This mechanism is evidently active in the present day, acidic groundwater regime, uranium presumably being mobilised as the carbonate complex. Although some evidence has been found of local re-precipitation, this is not considered to be volumetrically significant.

9. Little indication has been found of appreciable mobilisation of thorium and REEs from the limestone, although the intrinsic levels are perhaps too low to allow adequate detection by the methods used in this study. It is to be noted that the organic-silt laminae within the limestone unit, and the enclosing Facies "B" lithologies, show appreciable enrichment in thorium and REEs as well as in uranium. Investigation of these is merited in order to assess them as possible source-terms in thorium/REEs analogue modelling as well as to study further their role in supergene release of uranium.

6. ACKNOWLEDGEMENTS

The authors wish to thank their colleagues in BGS for their assistance and encouragement during the course of this research. In particular, Drs. P.J. Hooker, J.M. West and T.K. Ball are thanked for their helpful advice and discussions. Dr W.E. Falck is also acknowledged for help with field sampling and measurement. Staff at the Scottish Universities Research and Reactor Centre, East Kilbride, are thanked for carrying out the irradiations for fission track work. Professor G. Kelling is thanked for his useful comments during the review of the draft report.

7. REFERENCES

- ARAKEL, A.V. & McCONCHIE, D. 1982. Classification and genesis of calcrete and gypsum lithofacies in paleodrainage systems of inland Australia and their relationship to carnotite mineralisation. *Journal of Sedimentary Petrology*, **52**, 1149-1170.
- BALL, T.K. & MILODOWSKI, A.E. 1989. The geological, geochemical, hydrogeological and topographical characteristics of the Broubster Natural Analogue Site, Caithness. Report Fluid Processes Research Group, British Geological Survey, **WE/89/37**.
- BASHAM, I.R. 1981. Some applications of autoradiographs in textural analysis of uranium-bearing samples - a discussion. *Economic Geology*, **76**, 994-997.
- BASHAM, I.R., BALL, T.K., BEDDOE-STEPHENS, B. & MICHIE, U.McL. 1982(a). Uranium-bearing accessory minerals in granite fertility : Methods of identification and evaluation. *Uranium Exploration Methods*, 385-397. Proceedings of Symposium, Paris, 1982. (OECD/IAEA).
- BASHAM, I.R., BALL, T.K., BEDDOE-STEPHENS, B. & MICHIE, U.McL. 1982(b). Uranium-bearing accessory minerals in granite fertility : Studies of granites from the British Isles. *Uranium Exploration Methods*, 398-411. Proceedings of Symposium, Paris, 1982. (OECD/IAEA).
- BASHAM, I.R., MILODOWSKI, A.E., HYSLOP, E.K. & PEARCE, J.M. 1989. The location of uranium in source rocks and sites of secondary deposition at the Needle's Eye natural analogue site, Dumfries and Galloway. Report Fluid Processes Research Group, British Geological Survey, **WE/89/56**.
- BAULD, J. 1981. Geomicrobiological role of cyanobacterial mats in sedimentary environments: production and preservation of organic matter. *BMR Journal of Australian Geology & Geophysics*, **6**, 307-317.

- BEVERIDGE, T.J., MELOCHE, J.D., FYFE, W.S. & MURRAY, R.G.E. 1983. Diagenesis of metals chemically complexed to bacteria: laboratory formation of metal phosphates, sulphides, and organic condensates in artificial sediments. *Applied and Environmental Microbiology*, **45**, 1094-1108.
- BLACKBOURN, G. 1981. Probable Old Red Sandstone conglomerates around Tongue and adjacent areas, north Sutherland. *Scottish Journal of Geology*, **17**, 103-118.
- BRITISH GEOLOGICAL SURVEY (BGS). 1985. 1: 50 000 geological sheet 115(E) Reay (Scotland), solid edition.
- CARLISLE, D. 1983. Concentration of uranium and vanadium in calcretes and gypcretes. in: Wilson, R.C.L. (editor), *Residual Deposits: surface related weathering processes and materials*. Geological Society Special Publication, **11**, 185-195.
- COLE, R.M. & POPKIN, T.J. 1981. Chapter 4; Electron Microscopy. in: Philipp, G. *Manual of methods for general bacteriology*, American Society for Microbiology, 34-51.
- DeDECKKER, P. 1988. Large Australian lakes during the last 20 million years: sites for petroleum source rock or metal ore deposition, or both? in: Fleet, A.J., Kelts, K. & Talbot, M.R. (editors), *Lacustrine Petroleum Source Rocks*. Geological Society Special Publication, **40**, 45-58.
- DEGENS, E.T. & VENUGOPALEN, I. 1982. In situ metal-staining of biological membranes in sediments. *Nature*, **298**, 262-264.
- DISNAR, J.R. 1981. Etude experimentale de la fixation de metaux par un materiau sedimentaire actuel d'origine algaire-- II. Fixation 'in vitro' de UO_2^{2+} , Cu^{2+} , Ni^{2+} , Zn^{2+} , Pb^{2+} , Co^{2+} , Mn^{2+} , ainsi que de VO_3^- , MoO_4^{2-} et GeO_3^{2-} . *Geochimica et Cosmochimica Acta*, **45**, 363-379.
- DONOVAN, R.N. 1973. Basin margin deposits of the Middle Old Red Sandstone at Dirlot Caithness. *Scottish Journal of Geology*, **9**, 203-211.
- DONOVAN, R.N. 1975. Devonian lacustrine limestones at the margin of the Orcadian Basin, Scotland. *Journal of the Geological Society, London*, **131**, 489-510.
- DONOVAN, R.N. 1978. Caithness. in: Friend, P.F. & Williams, B.P.J. (editors). *Field guide to Devonian of Scotland, the Welsh Borderlands and South Wales*. Palaeontological Association, 37-53.
- DONOVAN, R.N. 1980. Lacustrine cycles, fish ecology and stratigraphic zonation in the Middle Devonian of Caithness. *Scottish Journal of Geology*, **16**, 35-50.
- DONOVAN, R.N. & COLLINS, A. 1978. Mound structures from the Caithness Flagstones (Middle Devonian), northern Scotland. *Journal of Sedimentary Petrology*, **48**, 171-174.
- DONOVAN, R.N. & FOSTER, R.J. 1972. Subaqueous shrinkage cracks from the Caithness Flagstone Series (Middle Devonian) of northeast Scotland. *Journal of Sedimentary Petrology*, **42**, 309-317.

- DONOVAN, R.N., FOSTER, R.J. & WESTOLL, T.S. 1974. A stratigraphical revision of the Old Red Sandstone of North-eastern Caithness. *Transactions of the Royal Society of Edinburgh*, **69**, 167-201.
- DUNCAN, A.D. & HAMILTON, R.F.M. 1988. Palaeolimnology and organic geochemistry of the Middle Devonian in the Orcadian Basin. in; Fleet, A.J., Kelts, K. & Talbot, M.R. (editors) *Lacustrine Petroleum Source Rocks*, Geological Society Special Publication, **40**, 173-201.
- FORTEY, N.J. & MICHIE, U.McL. 1978. Aegerine of possible authigenic origin in Middle Devonian sediments in Caithness, Scotland. *Mineralogical Magazine*, **42**, 439-442.
- GALLAGHER, M.J., MICHIE, U.McL., SMITH, R.T. & HAYNES, L. 1971. New evidence of uranium and other mineralization in Scotland. *Transactions of the Institute of Mining and Metallurgy*, **80B**, 150-173.
- GROVER, G. & READ, J.F. 1983. Paleoaquifer and deep burial related cements defined by regional cathodoluminescent patterns, middle Ordovician carbonates, Virginia. *Bulletin American Association of Petroleum Geologists*, **67**, 1275-1303.
- HUGGETT, J.M. 1984. An SEM study of phyllosilicates in a Westphalian coal measures sandstone using back-scattered electron imaging and wavelength dispersive spectral analysis. *Sedimentary Geology*, **40**, 233-247.
- KENT, P.E. 1975. Review of North Sea Basin development. *Journal of the Geological Society, London*, **131**, 435-468.
- KLEEMAN, J.D. & LOVERING, J.F. 1967. Uranium distribution in rocks by fission track registration in Lexan plastic prints. *Atomic Energy Australia*, **10**, No.4, 3-8.
- KRINSLEY, D.H., PYE, K. & KEARSLEY, A.T. 1983. Application of backscattered electron microscopy in shale petrology. *Geological Magazine*, **120**, 109-118.
- MARSHALL, J.E.A., BROWN, J.F. & HINDMARSH, S. 1985. Hydrocarbon source rock potential of the Devonian rocks of the Orcadian Basin. *Scottish Journal of Geology*, **21**, 301-320.
- MEYERS, W.J. 1974. Carbonate cement stratigraphy of the Lake Valley Formation (Mississippian) Sacramento Mountains, New Mexico. *Journal of Sedimentary Petrology*, **44**, 837-861.
- MICHIE, U. McL. & COOPER, D.C. 1979. Uranium in the Old Red Sandstone of Orkney. *Report Institute of Geological Sciences*, **78/16**.
- MILODOWSKI, A.E. & HURST, A. 1989. The authigenesis of phosphate minerals in some Norwegian hydrocarbon reservoirs; evidence for the mobility and redistribution of rare earth elements (REE) and Th during sandstone diagenesis. *Proceedings, Sixth International Symposium on Water-Rock Interaction (WRI 6)*, Malvern, UK, 3-12th August 1989.
- MYKURA, W. 1983. Old Red Sandstone. in *Geology of Scotland* (G.Y. Craig, editor), Chapter 8, 205-251.

- NICKEL, E. 1978. The present status of cathode luminescence as a tool in sedimentology. *Minerals Science Engineering*, **10**, 73-100.
- NORTON, M.G., McCLAY, K.R. & WAY, N.A. 1987. Tectonic evolution of Devonian basins in northern Scotland and southern Norway. *Norsk Geologisk Tidsskrift*, **67**, 323-338.
- PARNELL, J. 1983. Ancient duricrusts and related rocks in perspective: a contribution from the Old Red Sandstone. in: Wilson, R.C.L. (editor). *Residual deposits: surface related weathering processes and materials*. Geological Society Special Publication, **11**, 197-209.
- PARNELL, J. 1985(a). Evidence for evaporites in the ORS of northern Scotland: replaced gypsum horizons in Easter Ross. *Scottish Journal of Geology*, **21**, 377-380.
- PARNELL, J. 1985(b). Uranium/rare earth enriched hydrocarbons in Devonian sandstones, northern Scotland. *Neues Jahrbuch fur Mineralogie Monatshefte*, **H3/1985**, 132-144.
- PARNELL, J. 1985(c). The distribution of uranium in kolm: evidence from backscattered electron imagery. *Geologiska Foreningens I Stockholm Forhandlingar*, **104**, 231-234.
- PARNELL, J. 1985(d). Hydrocarbon source rocks, reservoir rocks and migration in the Orcadian Basin. *Scottish Journal of Geology*, **21**, 321-336.
- PARNELL, J. 1988. Significance of lacustrine cherts for the environment of source-rock deposition in the Orcadian Basin, Scotland. in: Fleet, A.J., Kelts, K. & Talbot, M.R. (editors). *Lacustrine petroleum source rocks*. Geological Society Special Publication, **40**, 205-217.
- PIERSON, B.J. 1981. The control of cathodoluminescence in dolomite by iron and manganese. *Sedimentology*, **28**, 601-610.
- PRETORIUS, D.A. 1975. The depositional environment of the Witwatersrand goldfields: a chronological review of speculations and observations. *Minerals Science and Engineering*, **7**, No.1, 18-47.
- PYE, K. & KRINSLEY, D.H. 1984. Petrographic examination of sedimentary rocks in the SEM using backscattered electron detectors. *Journal of Sedimentary Petrology*, **54**, 877-888.
- RENFRO, A.R. 1974. Genesis of evaporite-associated stratiform metalliferous deposits - a sabkha process. *Economic Geology*, **69**, 33-45.
- SCHIMDT, V. & McDONALD, D.A. 1979. The role of secondary porosity in the course of sandstone diagenesis. in: Scoble, P.A. & Schluger, P.R. (editors). *Aspects of Diagenesis*. Society of Economic Paleontologists and Mineralogists Special Publication, **26**, 175-207.
- SIPPEL, R.F. 1968. Sandstone petrology, evidence from luminescence petrography. *Journal of Sedimentary Petrology*, **38**, 530-554.

- SMITH, B., STUART, M., VICKERS, B. & PEACHEY, D. 1989. The characterisation of organics from the natural analogue site at Broubster, Caithness, Scotland. Report, Fluid Processes Research Group, British Geological Survey. WE/89/33.
- STOREY, B.C. & LINTERN, B.C. 1981. Geochemistry of the rocks of the Strath Halladale Aultnabreac District. British Geological Survey, Environmental Protection Unit Report ENPU 81-12.
- STRONG, G.E. & MILODOWSKI, A.E. 1987. Aspects of diagenesis of the Sherwood Sandstones of the Wessex Basin and their influence on reservoir characteristics. in: Marshall, J.D. (editor). Diagenesis of Sedimentary Sequences. Geological Society Special Publication, 36, 325-337.
- TEN HAVE, A.H.M. & HEIJNEN, W. 1985. Cathodoluminescence activation and zonation in carbonate rocks: an experimental approach. Geologie en Mijnbouw, 64, 297-310.
- TWEEDIE, J.R. 1979. Origin of uranium and other metal enrichments in the Helmsdale Granite, eastern Sutherland, Scotland. Transactions of the Institution of Mining and Metallurgy, 88, B145-153.
- TWEEDIE, J.R. 1981. The origin of uranium and other metal concentrations in the Helmsdale Granite and the Devonian sediments of the northeast of Scotland. PhD. thesis, University of Aberdeen.
- WALKER, G., ABUMERE, O.E. & KAMALUDDIN, B. 1989. Luminescence spectroscopy of Mn²⁺ centres in rock-forming carbonates. Mineralogical Magazine, 53, 201-211.
- WILSON, M.J. 1971. Clay mineralogy of the Old Red Sandstone (Devonian) of Scotland. Journal of Sedimentary Petrology, 41, 995-1007.

European Communities — Commission

**EUR 13280 — The uranium source-term mineralogy and geochemistry
at the Broubster natural analogue site, Caithness**

A. E. Milodowski, I. R. Basham, E. K. Hyslop, J. M. Pearce

Luxembourg: Office for Official Publications of the European Communities

1991 — X, 50 pp., num. tab., fig. — 21.0 x 29.7 cm

Nuclear science and technology series

ISBN 92-826-2420-X

Catalogue number: CD-NA-13280-EN-C

Price (excluding VAT) in Luxembourg: ECU 6.25

The British Geological Survey (BGS) has been conducting a coordinated research programme at the Broubster natural analogue site in Caithness, north Scotland. This work on a natural radioactive geochemical system has been carried out with the aim of improving our confidence in using predictive models of radionuclide migration in the geosphere. This report is one of a series being produced and it concentrates on the mineralogical characterization of the uranium distribution in the limestone unit considered as the 'source-term' in the natural analogue model.



Venta y suscripciones • Salg og abonnement • Verkauf und Abonnement • Πωλήσεις και συνδρομές
Sales and subscriptions • Vente et abonnements • Vendita e abbonamenti
Verkoop en abonnementen • Venda e assinaturas

BELGIQUE / BELGIË

Moniteur belge / Belgisch Staatsblad
Rue de Louvain 42 / Leuvenseweg 42
1000 Bruxelles / 1000 Brussel
Tél. (02) 512 00 26
Fax 511 01 84
CCP / Postrekening 000-2005502-27

Autres distributeurs /
Overige verkooppunten

Librairie européenne/ Europese Boekhandel
Avenue Albert Jonnart 50 /
Albert Jonnartlaan 50
1200 Bruxelles / 1200 Brussel
Tél. (02) 734 02 81
Fax 735 08 60

Jean De Lannoy

Avenue du Roi 202 /Koningslaan 202
1060 Bruxelles / 1060 Brussel
Tél. (02) 538 51 69
Télex 63220 UNBOOK B
Fax (02) 538 08 41

CREDOC

Rue de la Montagne 34 / Bergstraat 34
Bte 11 / Bus 11
1000 Bruxelles / 1000 Brussel

DANMARK

J. H. Schuitz Information A/S

EF-Publikationer

Ottillavej 18
2500 Valby
Tlf. 36 44 22 66
Fax 36 44 01 41
Girokonto 6 00 08 86

BR DEUTSCHLAND

Bundesanzeiger Verlag

Breite Straße
Postfach 10 80 06
5000 Köln 1
Tel. (02 21) 20 29-0
Fernschreiber:
ANZEIGER BONN 8 882 595
Fax 20 29 278

GREECE

G.C. Eleftheroudakis SA

International Bookstore
Nikis Street 4
10563 Athens
Tel. (01) 322 63 23
Telex 219410 ELEF
Fax 323 98 21

ESPAÑA

Boletín Oficial del Estado

Trafalgar, 27
28010 Madrid
Tel. (91) 44 82 135

Mundi-Prensa Libros, S.A.

Castelló, 37
28001 Madrid
Tel. (91) 431 33 99 (Libros)
431 32 22 (Suscripciones)
435 36 37 (Direccion)

Télex 49370-MPLI-E
Fax (91) 575 39 98

Sucursal:

Librería Internacional AEDOS
Consejo de Ciento, 391
08009 Barcelona
Tel. (93) 301 86 15
Fax (93) 317 01 41

Libreria de la Generalitat de Catalunya

Rambla dels Estudis, 118 (Palau Moja)
08002 Barcelona
Tel. (93) 302 68 35
302 64 82
Fax 302 12 99

FRANCE

Journal officiel Service des publications des Communautés européennes

26, rue Desaix
75727 Paris Cedex 15
Tél. (1) 40 58 75 00
Fax (1) 40 58 75 74

IRELAND

Government Publications Sales Office

Sun Alliance House
Molesworth Street
Dublin 2
Tel. 71 03 09

or by post

Government Stationery Office

EEC Section

6th floor
Bishop Street
Dublin 8
Tel. 78 16 66
Fax 78 06 45

ITALIA

Licosa Spa

Via Benedetto Fortini, 120/10
Casella postale 552
50125 Firenze
Tel. (055) 64 54 15
Fax 64 12 57
Telex 570466 LICOSA I
CCP 343 509

Subagenti:

Libreria scientifica Lucio de Biasio - AEIOU

Via Meravigli, 16
20123 Milano
Tel. (02) 80 76 79

Herder Editrice e Libreria

Piazza Montecitorio, 117-120
00186 Roma
Tel. (06) 679 46 28/679 53 04

Libreria giuridica

Via XII Ottobre, 172/R
16121 Genova
Tel. (010) 59 56 93

GRAND-DUCHÉ DE LUXEMBOURG

Abonnements seulement
Subscriptions only
Nur für Abonnements

Messageries Paul Kraus

11, rue Christophe Plantin
2339 Luxembourg
Tél. 499 88 88
Télex 2515
Fax 499 88 84 44
CCP 49242-63

NEDERLAND

SDU Overheidsinformatie

Externe Fondsen
Postbus 20014
2500 EA 's-Gravenhage
Tel. (070) 37 89 911
Fax (070) 34 75 778

PORTUGAL

Imprensa Nacional

Casa da Moeda, EP
Rua D. Francisco Manuel de Melo, 5
P-1092 Lisboa Codex
Tel. (01) 69 34 14

Distribuidora de Livros Bertrand, Ld.ª

Grupo Bertrand, SA

Rua das Terras dos Vales, 4-A
Apartado 37
P-2700 Amadora Codex
Tel. (01) 49 59 050
Telex 15798 BERDIS
Fax 49 60 255

UNITED KINGDOM

HMSO Books (PC 16)

HMSO Publications Centre
51 Nine Elms Lane
London SW8 5DR
Tel. (071) 873 9090
Fax GP3 873 8463
Telex 29 71 138

Sub-agent:

Alan Armstrong Ltd

2 Arkwright Road
Reading, Berks RG2 0SQ
Tel. (0734) 75 18 55
Telex 849937 AAALTD G
Fax (0734) 75 51 64

ÖSTERREICH

Manz'sche Verlags- und Universitätsbuchhandlung

Kohlmarkt 16
1014 Wien
Tel. (0222) 531 61-0
Telex 11 25 00 BOX A
Fax (0222) 531 61-81

SVERIGE

BTJ

Box 200
22100 Lund
Tel. (046) 18 00 00
Fax (046) 18 01 25

SCHWEIZ / SUISSE / SVIZZERA

OSEC

Stampfenbachstraße 85
8035 Zürich
Tel. (01) 365 51 51
Fax (01) 365 54 11

YUGOSLAVIA

Privredni Vjesnik

Bulevar Lenjina 171/XIV
11070 - Beograd
Tel. 123 23 40

TÜRKIYE

Pres Dagitim Ticaret ve sanayi A.Ş

Narlibahçe Sokak No. 15
Cağaloğlu
Istanbul
Tel. 512 01 90
Telex 23822 DSVO-TR

AUTRES PAYS
OTHER COUNTRIES
ANDERE LÄNDER

Office des publications officielles des Communautés européennes

2, rue Mercier
L-2985 Luxembourg
Tel. 49 92 81
Telex PUBOF LU 1324 b
Fax 48 85 73
CC bancaire BIL 8-109/6003/700

CANADA

Renouf Publishing Co. Ltd

Mail orders — Head Office:
1294 Algoma Road
Ottawa, Ontario K1B 3W8
Tel. (613) 741 43 33
Fax (613) 741 54 39
Telex 0534783

Ottawa Store:

61 Sparks Street
Tel. (613) 238 89 85

Toronto Store:

211 Yonge Street
Tel. (416) 363 31 71

UNITED STATES OF AMERICA

UNIPUB

4611-F Assembly Drive
Lanham, MD 20706-4391
Tel. Toll Free (800) 274 4888
Fax (301) 459 0056

AUSTRALIA

Hunter Publications

58A Gipps Street
Collingwood
Victoria 3066

JAPAN

Kinokuniya Company Ltd

17-7 Shinjuku 3-Chome
Shinjuku-ku
Tokyo 160-91
Tel. (03) 3439-0121

Journal Department

PO Box 55 Chitose
Tokyo 156
Tel. (03) 3439-0124

NOTICE TO THE READER

All scientific and technical reports published by the Commission of the European Communities are announced in the monthly periodical '**euro abstracts**'. For subscription (1 year: ECU 92) please write to the address below.

CD-NA-13280-EN-C

Price (excluding VAT) in Luxembourg: ECU 6.25



OFFICE FOR OFFICIAL PUBLICATIONS
OF THE EUROPEAN COMMUNITIES

L-2985 Luxembourg

ISBN 92-826-2420-X

